

Thermodynamic Geometry of Nonequilibrium Fluctuations in Cyclically Driven Transport

Zi Wang and Jie Ren*

Center for Phononics and Thermal Energy Science, China-EU Joint Lab on Nanophononics,
Shanghai Key Laboratory of Special Artificial Microstructure Materials and Technology,
School of Physics Science and Engineering, Tongji University, Shanghai 200092, China

(Dated: March 15, 2024)

Nonequilibrium thermal machines under cyclic driving generally outperform steady-state counterparts. However, there is still lack of coherent understanding of versatile transport and fluctuation features under time modulations. Here, we formulate a theoretical framework of thermodynamic geometry in terms of full counting statistics of nonequilibrium driven transports. We find that, besides the conventional dynamic and adiabatic geometric curvature contributions, the generating function is divided into an additional nonadiabatic contribution, manifested as the metric term of full counting statistics. This nonadiabatic metric generalizes recent results of thermodynamic geometry in near-equilibrium entropy production to far-from-equilibrium fluctuations of general currents. Furthermore, the framework proves geometric thermodynamic uncertainty relations of near-adiabatic thermal devices, constraining fluctuations in terms of statistical metric quantities. We exemplify the theory in experimentally accessible driving-induced quantum chiral transport and Brownian heat pump.

Introduction.—In the past decade, significant advances have been achieved in both experiments and theories that allow for direct manipulations of thermodynamics of small setups [1–9]. These systems are subject to large fluctuations that are detrimental to their stable output. Recently, it has been shown that cyclically driven thermal devices can be tuned to be more stable and perform better than their steady state counterparts [10–12], igniting a surge of interest into the stochastic thermodynamics of this regime.

The concept of geometry provides deep insights into the nonequilibrium cyclic driving. Its manifestation in transport was originally introduced in the Thouless pump, relating the quantization of pumped charge with the overall integral of the underlying non-trivial Berry curvature [13, 14]. This idea also generalizes to open systems [15–17]. In thermal devices, the geometric-phase-like contribution provides a way of directing heat flow [18–27] and constructing heat engines [28–31]. These geometric results, ranging from quantum Markovian systems to classical diffusive dynamics, are mainly restricted to the adiabatic slow driving protocols. By utilizing controls, nonadiabatic pump effect can be eliminated at the expense of extra dissipation [32, 33]. The leading order nonadiabatic dissipation in the finite but small driving frequency regime [34] is captured by the concept of thermodynamic metric [35–38]. Yet, in the arbitrarily fast regime, the average entropy production assumes another geometric interpretation that is lower bounded by the Wasserstein distance [39–42], providing insights into the optimal control of the dissipation during finite-time processes [43–45]. The above thermodynamic metric structures, defined on the probability manifold, make the derivation of efficiency-power trade-off [31, 46–48] and the optimal protocol design [49–61] straightforward.

However, previous nonadiabatic results based on the metric structure are merely restricted to the analysis of average work or entropy production without temperature bias. This leads to little understanding of the generic transport behaviors in open systems with multiple reservoirs and strong nonequilibrium bias, let alone the transport fluctuations thereof. Therefore,

important questions arise naturally: How to analyze general currents and fluctuations in nonadiabatic cyclic thermal devices? Can the nonadiabatic driven transport be characterized by a nonequilibrium thermodynamic metric structure? If so, what are the general constraints on transport fluctuations caused thereby?

In this Letter, we solve the problems by formulating a geometric scheme of the generating function of currents, representing the nonadiabatic effects on each order of current moments as a metric term of full counting statistics. Based on this statistical metric structure of nonequilibrium transport, we derive geometric thermodynamic uncertainty relations (Geometric TURs) to constrain the current fluctuations under the near-adiabatic driving in terms of statistical metric quantities. Originally, TUR was proposed [62] and proved theoretically [63, 64] and experimentally [65, 66] within the steady states of classical Markovian dynamics, which bounds the precision of fluctuating current Q in terms of the entropy production. TUR was subsequently generalized to the finite-time regime [67–69], quantum systems endowed with coherence effects [70–72], setups with broken time-reversal symmetry [73, 74], and even systems with feedback controls [68, 75]. Also, the well established fluctuation theorems [76, 77] prove the fluctuation theorem uncertainty relations [78]. For reviews on TUR, see Ref. [79]; for subsequent applications to the thermodynamic inference, see Refs. [80–82]. Importantly, Koyuk, Seifert and Pietzonka have derived a set of modified TURs, applicable to driven systems, by taking into account of the dependence of currents on the driving frequency [83–85].

Our results in this Letter advance the understanding of nonadiabatic geometric effects in parametrically driven thermal devices, which can be far from equilibrium. This allows for a study of fluctuating devices with various thermal functionalities regarding both average performance and fluctuation strength, paving the way towards designing precise thermal devices under non-equilibrium reservoirs and non-adiabatic cyclic modulations.

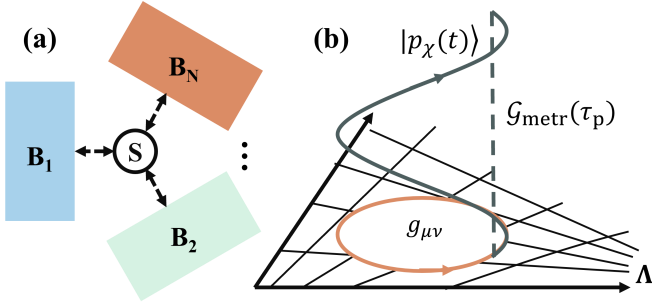


FIG. 1. **The metric geometry in cyclically driven transport.** (a) The nonequilibrium cyclically driven system S coupled to multiple reservoirs B_ν ($\nu = 1, 2, \dots, N$). (b) The metric structure of the cumulant generating function (CGF) $\mathcal{G}_{\text{metr}}(\tau_p) = \int_0^{\tau_p} dt g_{\mu\nu} \dot{\Lambda}_\mu \dot{\Lambda}_\nu$ in the curved parameter space Λ . The dashed line represents a metric CGF contribution $\mathcal{G}_{\text{metr}}(t)$ to the twisted distribution $|p_\chi(t)\rangle$ and describes the fluctuations in the nonadiabatic regime with an arbitrary driving speed, with χ being an auxiliary counting parameter for the interested current.

Setups.—We consider a cyclically driven open system coupled to multiple reservoirs B_ν , which is schematically shown in Fig. 1(a). The protocol parametrized as $\Lambda(t + \tau_p) = \Lambda(t)$ forms a closed curve $\partial\Omega$ in the parameter space Λ , with τ_p being the driving period. Without loss of generality, we here take the discrete state case as an example. Similar discussions also apply for continuous cases. As such, the system distribution function is $|p(t)\rangle := (p_1, \dots, p_N)^T$, with p_i ($1 \leq i \leq N$) describing the probability of occupying state i . The transition rate along $j \rightarrow i$ induced by the ν -th reservoir is k_{ij}^ν ($i \neq j$), which can be time dependent under the protocol $\Lambda(t)$. The master equation is thus written as $\partial_t |p(t)\rangle = \hat{L}(t) |p(t)\rangle$ with $L_{ij} = \sum_\nu (k_{ij}^\nu - \delta_{ij} \sum_{l \neq i} k_{li}^\nu)$ conserving the probability during transitions by $\sum_i L_{ij} = 0$.

To each transition path k_{ij}^ν , we associate an increment of the accumulated current $\Delta Q = d_{ij}^\nu$ [79]. Stochastic exchanges between the system and reservoirs, like the current of particle number, heat, or work, are described by the antisymmetric tensor $d_{ij}^\nu = -d_{ji}^\nu$. While, the symmetric $d_{ij}^\nu = d_{ji}^\nu$ corresponds to time-reversal invariant quantities like dynamic activity ($d_{ij}^\nu = 1$) [86]. The evolution of the full counting statistics of accumulated currents can be considered by the twisted operator \hat{L}_χ with the counting field χ :

$$\partial_t |p_\chi(t)\rangle = \hat{L}_\chi(t) |p_\chi(t)\rangle, \quad (1)$$

where the matrix elements are $L_{\chi,ij} = \sum_\nu k_{ij}^\nu e^{\chi d_{ij}^\nu}$ for $i \neq j$ and $L_{\chi,ii} = L_{ii}$. By defining the cumulant generating function (CGF) $\mathcal{G} := \ln \mathcal{Z} = \ln \langle 1 | p_\chi(t) \rangle$, the n -th cumulant of stochastic accumulated current Q at time t is obtained by taking the n -order derivative of CGF with respect to χ , as $\langle Q^n \rangle_c = \partial_\chi^n \mathcal{G}|_{\chi=0}$. Here, $\langle 1 |$ is a vector with all elements being 1 and \mathcal{Z} is the moment generating function encoding each order of moments by $\langle Q^n \rangle = \partial_\chi^n \mathcal{Z}|_{\chi=0}$. The non-Hermitian \hat{L}_χ can be decomposed into $\hat{L}_\chi = \sum_{n=0}^N E_n |r_n\rangle \langle l_n|$, where the left and right eigenvectors are biorthogonal $\langle l_m | r_n \rangle =$

$\delta_{m,n}$ and $n = 0$ corresponds to the unique steady state (we assume the ground state of \hat{L}_χ is nondegenerate). For details of the dynamics of the twisted master equation, see Sec. I of [87].

Thermodynamic Geometry of Full Counting Statistics.—Here, we sketch the derivation scheme of our most general geometric formulation. For derivation details, see Sec. II of [87]. Supposing that after several driving cycles, the system enters its cyclic state, satisfying the Floquet theorem

$$|p_\chi(t)\rangle = e^{\mathcal{G}(t)} |\phi(t)\rangle = e^{\mathcal{G}_{\text{dyn}}(t) + \mathcal{G}_{\text{geo}}(t)} |\phi(t)\rangle, \quad (2)$$

where $|\phi(t + \tau_p)\rangle = |\phi(t)\rangle$ is a cyclic state and $|p_\chi(t)\rangle$ only accumulates a CGF $\mathcal{G}(\tau_p) = \mathcal{G}_{\text{dyn}}(\tau_p) + \mathcal{G}_{\text{geo}}(\tau_p)$ during one driving period. It shows clearly that in addition to the dynamic-phase-like steady states contribution $\mathcal{G}_{\text{dyn}}(\tau_p) := \int_0^{\tau_p} dt E_0(t)$, there is a general geometric contribution

$$\mathcal{G}_{\text{geo}}(\tau_p) = - \oint_{\partial\Omega} d\Lambda_\mu \langle l_0 | \partial_\mu \phi(t) \rangle, \quad (3)$$

where we define $\partial_\mu := \partial_{\Lambda_\mu}$ for short. \mathcal{G}_{geo} is formally analogous to the Aharonov-Anandan phase in driven quantum systems [88], containing both the adiabatic and nonadiabatic effects. \mathcal{G}_{dyn} is simply an average over instantaneous steady states, while \mathcal{G}_{geo} has no static analogues. Specifically, one can decompose the state $|\phi\rangle$ into the adiabatic and nonadiabatic components, which are respectively the instantaneous steady state $|r_0\rangle$ and the transverse states perpendicular to $|r_0\rangle$, as:

$$|\phi(t)\rangle = |r_0(t)\rangle + \hat{G} |\partial_t \phi(t)\rangle, \quad (4)$$

where the operator $\hat{G} := (\hat{L}_\chi - E_0)^+ (\hat{1} - |\phi\rangle \langle l_0|)$, with the pseudo-inverse $(\hat{L}_\chi - E_0)^+ = \sum_{n \neq 0} \frac{1}{E_n - E_0} |r_n\rangle \langle l_n|$. The first term is the adiabatic trajectory and the second term signifies the non-adiabatic excitations.

By substituting Eq. (4) into Eq. (3), we find that the geometric CGF is generally divided into two parts: $\mathcal{G}_{\text{geo}} = \mathcal{G}_{\text{curv}} + \mathcal{G}_{\text{metr}}$. The first part is the adiabatic Berry-curvature-like CGF $\mathcal{G}_{\text{curv}} = \oint_{\partial\Omega} d\Lambda_\mu A_\mu = \int_\Omega dS_{\mu\nu} F_{\mu\nu}$ [18, 24, 26, 28–30] with the geometric connection $A_\mu = -\langle l_0 | \partial_\mu r_0 \rangle$ and the antisymmetric curvature $F_{\mu\nu} = \langle \partial_\nu l_0 | \partial_\mu r_0 \rangle - \langle \partial_\mu l_0 | \partial_\nu r_0 \rangle$, governing the current statistics in the adiabatic regime. This regime is fertile in constructing precise and efficient adiabatic thermal machines [9–12].

Of our prime interest is actually the second part, the nonadiabatic metric component:

$$\mathcal{G}_{\text{metr}}(\tau_p) = \int_0^{\tau_p} g_{\mu\nu} \dot{\Lambda}_\mu \dot{\Lambda}_\nu dt, \quad (5)$$

$$\text{with } g_{\mu\nu} := \frac{1}{2} \left[\langle \partial_\mu l_0 | \hat{G} | \partial_\nu \phi \rangle + \langle \partial_\nu l_0 | \hat{G} | \partial_\mu \phi \rangle \right],$$

from which the full nonadiabatic effect on each order of fluctuation cumulants can be derived $\langle Q^n_{\text{metr}} \rangle_c := \partial_\chi^n \mathcal{G}_{\text{metr}}|_{\chi=0} = \int_0^{\tau_p} g_{\mu\nu}^Q \dot{\Lambda}_\mu \dot{\Lambda}_\nu dt$, with the corresponding metric for cumulants being $g_{\mu\nu}^Q := \partial_\chi^n g_{\mu\nu}|_{\chi=0}$. This metric structure in CGF is illustrated in Fig. 1(b). In contrast to

the time-antisymmetric $\mathcal{G}_{\text{curv}}$ that reverses upon time reversal, the time-symmetric metric tensor (also symmetric in the sense of $g_{\mu\nu} = g_{\nu\mu}$) indicates that the nonadiabatic component $\mathcal{G}_{\text{metr}}$ provides a time-reversal invariant contribution of each current and the corresponding fluctuations. We note that although Eq. (5) is merely a formal solution, our following concrete results follow from it.

The statistical metric Eq. (5) describes the full non-adiabatic effect on arbitrary transport fluctuations. In the near-adiabatic regime, the state $|\phi(t)\rangle$ reduces to $|r_0(t)\rangle$ and the metric simplifies to the leading order of nonadiabaticity, as

$$\mathfrak{g}_{\mu\nu} = \sum_{n \neq 0} \frac{\langle \partial_\mu l_0 | r_n \rangle \langle l_n | \partial_\nu r_0 \rangle + (\mu \leftrightarrow \nu)}{2(E_n - E_0)}, \quad (6)$$

which describes the near-adiabatic currents and fluctuations. Here, $(\mu \leftrightarrow \nu)$ means interchanging indices. Previous works on the thermodynamic geometry can be derived by restricting to this near-equilibrium regime and consider only the average entropy production [36, 38, 47] or its fluctuation [51] in setups with a single reservoir.

It is worth noting that, in the geometry of optimal transport, the cost of changing between distributions, i.e., the average entropy production, is determined by other metrics on the probability manifold [40–42], both for the overdamped [39, 43], underdamped Brownian [45] and discrete master equation case [42, 44]. The minimization of average entropy production naturally reduces to finding the geodesic between initial and final distributions, whose length is bounded from below by the Wasserstein distance [39, 42], leading to the optimal Landauer erasure [39, 53, 61]. Distinct from the above regime, the metric Eq. (5) here works in the geometry of parameter space, which is valid for any currents and fluctuations of interest under cyclic parametric driving. In what follows, we will discuss implications of the statistical metric of CGF on average currents and fluctuations, separately.

Metric Structure and Average Currents.—Here, we consider consequences of the CGF metric on the average current. Details of calculation are summarized in Sec. III of [87]. We show that the average current during one period is $\langle Q \rangle := \partial_\chi \mathcal{G}(\tau_p)|_{\chi=0} = \int_0^{\tau_p} dt \langle 1 | \hat{J}(t) | p(t) \rangle$, with the current operator being $\hat{J} := \partial_\chi \hat{L}_\chi|_{\chi=0}$ and the cyclic distribution being $|p(t)\rangle = |p_\chi(t)\rangle|_{\chi=0}$. Particularly, we derive the nonadiabatic metric structure for current Q , as:

$$\langle Q_{\text{metr}} \rangle := \partial_\chi \mathcal{G}_{\text{metr}}(\tau_p)|_{\chi=0} = \int_0^{\tau_p} g_{\mu\nu}^Q \dot{\Lambda}_\mu \dot{\Lambda}_\nu dt, \quad (7)$$

$$\text{with } g_{\mu\nu}^Q = \frac{1}{2} \left[\langle 1 | \hat{J} \hat{L}^+ \partial_\mu (\hat{L}^+ | \partial_\nu p) \rangle + (\mu \leftrightarrow \nu) \right],$$

where $g_{\mu\nu}^Q = \partial_\chi g_{\mu\nu}|_{\chi=0}$ is a symmetric metric with respect to the average accumulated current $\langle Q \rangle$ and \hat{L}^+ is the pseudo-inverse of $\hat{L}_\chi|_{\chi=0}$. It is worth noting that Eq. (7) works for arbitrary nonadiabatic driving speed. If one replaces $|p\rangle$ by the instantaneous steady states $|\pi\rangle$ in Eq. (7), one will enter in the near-adiabatic regime and obtain the corresponding met-

ric $\mathfrak{g}_{\mu\nu}^Q = \left[\langle 1 | \hat{J} \hat{L}^+ \partial_\mu (\hat{L}^+ | \partial_\nu \pi) \rangle + (\mu \leftrightarrow \nu) \right] / 2$, which describes the leading order finite-time effect.

Here, we discuss the application of Eq. (7) to thermodynamic optimization. The metric of total entropy production can be expressed as $\tilde{g}_{tt} = g_{tt}^\Sigma + \partial_t(\sigma_p - \sigma_\pi)$, where g_{tt}^Σ describes the reservoir entropy production due to heat currents and $\partial_t(\sigma_p - \sigma_\pi)$ is the system entropy production rate, with $\sigma_p = -\sum_n p_n \ln p_n$. Note that over one whole period, $\langle \Sigma \rangle := \int_0^{\tau_p} dt g_{tt}^\Sigma = \int_0^{\tau_p} dt \tilde{g}_{tt}$ since $|p\rangle$ and $|\pi\rangle$ is cyclic in time. The positivity of total entropy production guarantees $\tilde{g}_{tt} > 0$, which allows us to obtain a thermodynamic speed limit $\tau_p \geq L^2 / \langle \Sigma \rangle$, bounding the system evolution speed with entropy production and non-equilibrium thermodynamic length $L = \int_0^{\tau_p} dt \sqrt{\tilde{g}_{tt}}$. The equality is obtained when the entropy production rate is constant and this endows us an entropy minimization principle $\partial_t \tilde{g}_{tt} = 0$.

We note that the pseudo-Riemannian-metric $g_{\mu\nu}^Q$ is not promised to be positive-definite. Nevertheless, this "non-positive definite" sacrifice allows us to generalize the previous thermodynamic geometry framework to non-equilibrium transports for generic currents in finite-time driving regimes. For example, in the near-adiabatic regime, we can obtain the vector field in the parameter space along which the non-adiabatic pump current vanishes $\mathfrak{g}_{\mu\nu}^Q \dot{\Lambda}^\mu \dot{\Lambda}^\nu = 0$. This provides us a geometric view point of the non-adiabatic control over the time-dependent pump effect. For details of this optimization principle, see Sec. IV of [87]. The concise average current expression Eq. (7) is simply a consequence of our general result Eq. (5), which generally encodes the statistical information of each order fluctuation cumulants $\langle Q_{\text{metr}}^n \rangle_c$.

Geometric TURs and Fluctuations.—Here, by restricting to the near-adiabatic regime, we show that the fluctuations encoded by Eq. (6) are constrained by a kind of Geometric TURs, wherein the two geometric terms originated from $\mathcal{G}_{\text{geo}} = \mathcal{G}_{\text{curv}} + \mathcal{G}_{\text{metr}}$ play a central role. Based on the fluctuation-response inequality [89], which is a nonlinear generalization of the Cramer-Rao bound, we obtain the Geometric TURs (see Sec. V of [87] for details), as:

$$\langle \Sigma \rangle \geq 2 \frac{(\langle Q_{\text{dyn}} \rangle - \langle Q_{\text{metr}} \rangle)^2}{\langle Q^2 \rangle_c} := \Sigma_g, \quad (8)$$

where Σ is the entropy production during one driving period, Q_{dyn} and Q_{metr} are respectively the dynamic and nonadiabatic metric components of an arbitrary time-antisymmetric current (that can be particle number, heat, or work). Both the variance $\langle Q^2 \rangle_c$ and entropy production $\langle \Sigma \rangle$ contain contributions of the dynamic, adiabatic curvature and nonadiabatic metric origins. Eq. (8), consistent with Ref. [84], generalizes the adiabatic limit results in a thermoelectric heat engine [90]. It clearly unveils the role played by the near-adiabatic metric structure and paves the way towards geometric inference and optimization.

Now let us show some direct consequences of the Geometric TURs on the near-adiabatic but finite-time processes. If the reservoirs are instantaneously isothermal with each other,

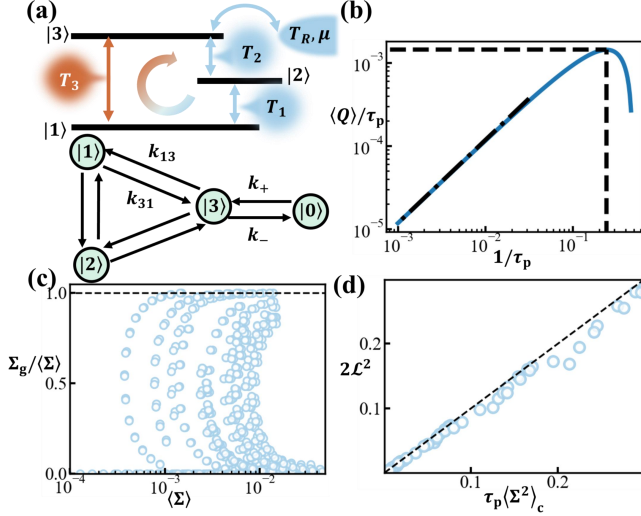


FIG. 2. **The nonequilibrium quantum tricycle model with energy levels ϵ_n of quantum dots being driven.** (a) The system setup and its transition graph. Three quantum dots with tunable energy levels are mediated by three thermal photonic/phononic reservoirs. The level $|3\rangle$ is in addition coupled to an electron reservoir. (b) The nonadiabatic average heat flux versus the inverse period ($\phi = 2\pi/3$ and $T_1 = T_2 = T_3 = T_R$). The dot-dash line is for the adiabatic component and the dash line is for the optimal period. (c) The geometric TUR ($\Sigma_g := 2(\langle Q_{\text{dyn}} \rangle - \langle Q_{\text{metr}} \rangle)^2 / \langle Q^2 \rangle_c$) is verified. (d) The geometric bound on the fluctuation of entropy production ($\langle \Sigma^2 \rangle_c \tau_p \geq 2\mathcal{L}^2$) is verified.

the dynamic components vanish in the sense of mean values $\langle Q_{\text{dyn}} \rangle = \langle \Sigma_{\text{dyn}} \rangle = 0$, but not necessary for the fluctuation $\langle Q_{\text{dyn}}^2 \rangle_c$ of an arbitrary current. Meanwhile, $\langle \Sigma_{\text{curv}} \rangle = 0$ due to the vanishing quasistatic entropy production. By rewriting Eq. (8) as $\langle Q^2 \rangle_c \geq 2(\langle Q_{\text{dyn}} \rangle - \langle Q_{\text{metr}} \rangle)^2 / (\langle \Sigma_{\text{dyn}} \rangle + \langle \Sigma_{\text{curv}} \rangle + \langle \Sigma_{\text{metr}} \rangle)$, we can obtain a geometric bound for the current fluctuation

$$\langle Q^2 \rangle_c \geq 2 \frac{\langle Q_{\text{metr}} \rangle^2}{\langle \Sigma_{\text{metr}} \rangle}, \quad (9)$$

which becomes tighter for faster drivings. By taking the entropy production as the current ($Q := \Sigma$) and considering the positive-definiteness of $g_{\mu\nu}^\Sigma$, we can bound the fluctuation of entropy production Σ by the thermodynamic length \mathcal{L} , as:

$$\langle \Sigma^2 \rangle_c \geq \frac{2\mathcal{L}^2}{\tau_p}, \quad (10)$$

where $\mathcal{L} := \oint_{\partial\Omega} \sqrt{g_{\mu\nu}^\Sigma d\Lambda_\mu d\Lambda_\nu}$ is a geometric quantity independent of the parametrization of protocol. Here, we use both Eq. (9) and the Cauchy-Schwarz inequality [36, 47]: $\langle \Sigma^2 \rangle_c \geq 2 \langle \Sigma_{\text{metr}} \rangle = 2 \int_0^{\tau_p} g_{\mu\nu}^\Sigma \dot{\Lambda}_\mu \dot{\Lambda}_\nu dt \geq 2\mathcal{L}^2/\tau_p$. This result can be understood as a kind of fluctuation-dissipation inequality. The geometric bound Eq. (10) connects the entropy production fluctuation in near-equilibrium finite-time processes to previously defined thermodynamic length [35, 36], providing

a basis for inferring the statistical distribution of entropy production in cyclically driven processes.

In the following, we will validate the metric structure Eq. (6) and the Geometric TURs [Eq. (8) and (10)] using two examples.

Discrete Master Equation System.—Our first model is the nonequilibrium quantum tricycle generating the chiral current by the cyclic driving, illustrated in Fig. 2(a), which is inspired by the classical stochastic pump model [17, 91] and steady-state continuous thermal devices [92]. The system Hamiltonian $\hat{H} = \hat{H}_S + \hat{H}_R + \hat{H}_{SR} + \hat{H}_B + \hat{H}_{SB}$ is composed of the three quantum dot levels $\hat{H}_S = \sum_{n=1}^3 \epsilon_n \hat{c}_n^\dagger \hat{c}_n$, the electron reservoirs $\hat{H}_R = \sum_k \epsilon_k \hat{d}_k^\dagger \hat{d}_k$, the tunneling term $\hat{H}_{SR} = \sum_k t_k (\hat{d}_k^\dagger \hat{c}_3 + \hat{c}_3^\dagger \hat{d}_k)$, the Bosonic thermal reservoir $\hat{H}_B = \sum_{\nu=1; k}^{\nu=3} \epsilon_{\nu, k} \hat{a}_{\nu, k}^\dagger \hat{a}_{\nu, k}$, and the system-reservoir coupling term $\hat{H}_{SB} = \sum_{\nu=1; k}^{\nu=3} r_{\nu, k} (\hat{a}_{\nu, k} + \hat{a}_{\nu, k}^\dagger) (\hat{c}_\nu^\dagger \hat{c}_{\nu+1} + \hat{c}_{\nu+1}^\dagger \hat{c}_\nu)$. Here, $\nu = 4$ denotes the same site as $\nu = 1$. \hat{H}_{SB} mediates the transitions between quantum dots $|i\rangle$ and $|i+1\rangle$ ($1 \leq i \leq 3$) and \hat{H}_{SR} enables electrons to hop into (out of) the system through the transition $|0\rangle \rightarrow |3\rangle$ ($|3\rangle \rightarrow |0\rangle$). We restrict ourselves to the Coulomb blockade and the weak coupling regime. For the twisted master equation and driving protocols, see Sec. VIA in [87].

By driving the energy level of quantum dots ϵ_n out of phase, e.g. $\epsilon_n(t) = \epsilon_n^0 + \delta \sin[2\pi t/\tau_p + (n-1)\phi]$ with δ being the driving amplitude, we realize the driving induced chiral current even in the absence of biases. As shown in Fig. 2(b), $\langle Q \rangle/\tau_p$ is decreased by the nonadiabatic effect and reaches its maximum $-\langle Q_{\text{curv}} \rangle^2 / (4\tau_p \langle Q_{\text{metr}} \rangle)$ at the optimal period $-2\tau_p \langle Q_{\text{metr}} \rangle / \langle Q_{\text{curv}} \rangle$ as denoted by the dashed lines. In contrast to the nonzero pumping, by merely driving the well depth (energy level) of the classical analog satisfying the Arrhenius law of transition rate, the chiral current is prohibited by the no-pumping theorem [17, 93]. As shown in Fig. 2(c), the average entropy production can be bounded and inferred by the chiral current fluctuations, satisfying Eq. (8). Also, as shown in Fig. 2(d), the fluctuation of the entropy production itself is bounded from left by the thermodynamic length, validating the geometric bound Eq. (10).

Continuous Brownian System.—Here, we show that Eq. (10) can be saturated in a Brownian heat pump engine. We consider two linearly coupled harmonic oscillators between two reservoirs of temperature T_i [19]. The Langevin dynamics is $\Gamma \dot{\mathbf{x}} = K \mathbf{x} + \boldsymbol{\xi}(t)$, where $\mathbf{x} = (x_1, x_2)^T$ is the oscillators' position and $\boldsymbol{\xi} = (\xi_1, \xi_2)^T$ is a vector of independent Gaussian white noise satisfying $\langle \xi_i \rangle = 0$, $\langle \xi_i(t_1) \xi_j(t_2) \rangle = 2\gamma_i T_i \delta_{ij} \delta(t_1 - t_2)$. The viscosity and stiffness matrices are $\Gamma = \begin{pmatrix} \gamma_1 & 0 \\ 0 & \gamma_2 \end{pmatrix}$, $K = k \begin{pmatrix} -1 & 1 \\ 1 & -1 \end{pmatrix}$.

By analytical calculation, when $\boldsymbol{\Lambda} = (k, \gamma_1)^T$ is driven, the metric for the average entropy production $g_{\mu\nu}^\Sigma$ and entropy variance $g_{\mu\nu}^{\Sigma^2}$ in the isothermal case ($T_1 = T_2$) satisfies $g_{\mu\nu}^{\Sigma^2} = 2g_{\mu\nu}^\Sigma$. Our bound Eq. (10) is saturable by reparametrizing the protocol in terms of the thermodynamic length, i.e., the time spent around a parameter point being

$dt = (\tau_p/\mathcal{L})\sqrt{g_{\mu\nu}^{\Sigma}d\Lambda_{\mu}d\Lambda_{\nu}}$ [36, 47]. For details, see the Sec. VIB of [87].

Summary.— We have proposed a general framework of thermodynamic geometry in terms of full counting statistics for analyzing the transport fluctuations in nonequilibrium driven systems. Our theory can study the fluctuation properties of arbitrary currents among multiple reservoirs under finite-time modulations. As an illustration, we have proved and validated the geometric TURs, relating the current fluctuations and entropy production in near-adiabatically driven systems. We have verified the results in a quantum chiral transport and Brownian heat pump, both analytically and numerically. This geometry framework can be readily adopted to study the effect of quantum phenomena (like quantum coherence [94–96], squeezing [97, 98]) on the performance and TUR of heat engines in the finite-time regime. Also, deriving optimal protocols with minimal fluctuations under cyclic parametric driving with arbitrary speed is an important future direction.

We acknowledge the support from the National Natural Science Foundation of China (No. 11935010), the Natural Science Foundation of Shanghai (Grant Nos. 23ZR1481200 and 23XD1423800), and the Opening Project of Shanghai Key Laboratory of Special Artificial Microstructure Materials and Technology.

* Corresponding Email: Xonics@tongji.edu.cn

- [1] Valentin Blickle and Clemens Bechinger, “Realization of a micrometre-sized stochastic heat engine,” *Nat. Phys.* **8**, 143–146 (2012).
- [2] J. Roßnagel, O. Abah, F. Schmidt-Kaler, K. Singer, and E. Lutz, “Nanoscale heat engine beyond the carnot limit,” *Phys. Rev. Lett.* **112**, 030602 (2014).
- [3] Ignacio A Martínez, Édgar Roldán, Luis Dinis, Dmitri Petrov, Juan MR Parrondo, and Raúl A Rica, “Brownian carnot engine,” *Nat. Phys.* **12**, 67–70 (2016).
- [4] Ignacio A Martínez, Artyom Petrosyan, David Guéry-Odelin, Emmanuel Trizac, and Sergio Ciliberto, “Engineered swift equilibration of a brownian particle,” *Nat. Phys.* **12**, 843–846 (2016).
- [5] Martin Josefsson, Artis Svilans, Adam M Burke, Eric A Hoffmann, Sofia Fahlvik, Claes Thelander, Martin Leijnse, and Heiner Linke, “A quantum-dot heat engine operating close to the thermodynamic efficiency limits,” *Nat. Nanotechnol.* **13**, 920–924 (2018).
- [6] Peter Talkner and Peter Hänggi, “Colloquium: Statistical mechanics and thermodynamics at strong coupling: Quantum and classical,” *Rev. Mod. Phys.* **92**, 041002 (2020).
- [7] Rongqian Wang, Chen Wang, Jincheng Lu, and Jian-Hua Jiang, “Inelastic thermoelectric transport and fluctuations in mesoscopic systems,” *Adv. Phys.-X* **7**, 2082317 (2022).
- [8] Tushar K Saha, Joseph NE Lucero, Jannik Ehrich, David A Sivak, and John Bechhoefer, “Maximizing power and velocity of an information engine,” *Proc. Natl. Acad. Sci. U.S.A* **118**, e2023356118 (2021).
- [9] Viktor Holubec and Artem Ryabov, “Fluctuations in heat engines,” *J. Phys. A Math. Theor.* **55**, 013001 (2021).
- [10] Andre C. Barato and Udo Seifert, “Cost and precision of brownian clocks,” *Phys. Rev. X* **6**, 041053 (2016).
- [11] Viktor Holubec and Artem Ryabov, “Cycling tames power fluctuations near optimum efficiency,” *Phys. Rev. Lett.* **121**, 120601 (2018).
- [12] Harry J. D. Miller, M. Hamed Mohammady, Martí Perarnau-Llobet, and Giacomo Guarneri, “Thermodynamic uncertainty relation in slowly driven quantum heat engines,” *Phys. Rev. Lett.* **126**, 210603 (2021).
- [13] D. J. Thouless, “Quantization of particle transport,” *Phys. Rev. B* **27**, 6083–6087 (1983).
- [14] Michael Victor Berry, “Quantal phase factors accompanying adiabatic changes,” *Proc. R. Soc. A* **392**, 45–57 (1984).
- [15] P. W. Brouwer, “Scattering approach to parametric pumping,” *Phys. Rev. B* **58**, R10135–R10138 (1998).
- [16] N. A. Sinitsyn and Ilya Nemenman, “Universal geometric theory of mesoscopic stochastic pumps and reversible ratchets,” *Phys. Rev. Lett.* **99**, 220408 (2007).
- [17] Saar Rahav, Jordan Horowitz, and Christopher Jarzynski, “Directed flow in nonadiabatic stochastic pumps,” *Phys. Rev. Lett.* **101**, 140602 (2008).
- [18] Jie Ren, Peter Hänggi, and Baowen Li, “Berry-phase-induced heat pumping and its impact on the fluctuation theorem,” *Phys. Rev. Lett.* **104**, 170601 (2010).
- [19] Jie Ren, Sha Liu, and Baowen Li, “Geometric heat flux for classical thermal transport in interacting open systems,” *Phys. Rev. Lett.* **108**, 210603 (2012).
- [20] Tatsuro Yuge, Takahiro Sagawa, Ayumu Sugita, and Hisao Hayakawa, “Geometrical pumping in quantum transport: Quantum master equation approach,” *Phys. Rev. B* **86**, 235308 (2012).
- [21] Tian Chen, Xiang-Bin Wang, and Jie Ren, “Dynamic control of quantum geometric heat flux in a nonequilibrium spin-boson model,” *Phys. Rev. B* **87**, 144303 (2013).
- [22] Chen Wang, Jie Ren, and Jianshu Cao, “Unifying quantum heat transfer in a nonequilibrium spin-boson model with full counting statistics,” *Phys. Rev. A* **95**, 023610 (2017).
- [23] Kota L. Watanabe and Hisao Hayakawa, “Geometric fluctuation theorem for a spin-boson system,” *Phys. Rev. E* **96**, 022118 (2017).
- [24] Wenjie Nie, Guoyao Li, Xiyun Li, Aixi Chen, Yueheng Lan, and Shi-Yao Zhu, “Berry-phase-like effect of thermo-phonon transport in optomechanics,” *Phys. Rev. A* **102**, 043512 (2020).
- [25] Zi Wang, Luqin Wang, Jiangzhi Chen, Chen Wang, and Jie Ren, “Geometric heat pump: Controlling thermal transport with time-dependent modulations,” *Front. Phys.* **17**, 13201 (2022).
- [26] Zi Wang, Jiangzhi Chen, and Jie Ren, “Geometric heat pump and no-go restrictions of nonreciprocity in modulated thermal diffusion,” *Phys. Rev. E* **106**, L032102 (2022).
- [27] Juliette Monsel, Jens Schulenburg, Thibault Baquet, and Janine Splettstoesser, “Geometric energy transport and refrigeration with driven quantum dots,” *Phys. Rev. B* **106**, 035405 (2022).
- [28] Sajal Kumar Giri and Himangshu Prabal Goswami, “Geometric phaselike effects in a quantum heat engine,” *Phys. Rev. E* **96**, 052129 (2017).
- [29] Bibek Bhandari, Pablo Terrén Alonso, Fabio Taddei, Felix von Oppen, Rosario Fazio, and Liliana Arrachea, “Geometric properties of adiabatic quantum thermal machines,” *Phys. Rev. B* **102**, 155407 (2020).
- [30] Yuki Hino and Hisao Hayakawa, “Geometrical formulation of adiabatic pumping as a heat engine,” *Phys. Rev. Research* **3**, 013187 (2021).
- [31] Hisao Hayakawa, Ville MM Paasonen, and Ryosuke Yoshii, “Geometrical quantum chemical engine,” [arXiv preprint](#)

arXiv:2112.12370 (2021).

- [32] Kazutaka Takahashi, Keisuke Fujii, Yuki Hino, and Hisao Hayakawa, “Nonadiabatic control of geometric pumping,” *Phys. Rev. Lett.* **124**, 150602 (2020).
- [33] Ken Funo, Neill Lambert, Franco Nori, and Christian Flindt, “Shortcuts to adiabatic pumping in classical stochastic systems,” *Phys. Rev. Lett.* **124**, 150603 (2020).
- [34] Bjarne Andresen, Peter Salamon, and R Stephen Berry, “Thermodynamics in finite time,” *Phys. Today* **37**, 62 (1984).
- [35] Peter Salamon and R. Stephen Berry, “Thermodynamic length and dissipated availability,” *Phys. Rev. Lett.* **51**, 1127–1130 (1983).
- [36] Gavin E. Crooks, “Measuring thermodynamic length,” *Phys. Rev. Lett.* **99**, 100602 (2007).
- [37] Edward H. Feng and Gavin E. Crooks, “Far-from-equilibrium measurements of thermodynamic length,” *Phys. Rev. E* **79**, 012104 (2009).
- [38] David A. Sivak and Gavin E. Crooks, “Thermodynamic metrics and optimal paths,” *Phys. Rev. Lett.* **108**, 190602 (2012).
- [39] Erik Aurell, Krzysztof Gawedzki, Carlos Mejía-Monasterio, Roya Mohayaee, and Paolo Muratore-Ginanneschi, “Refined second law of thermodynamics for fast random processes,” *J. Stat. Phys.* **147**, 487 (2012).
- [40] Muka Nakazato and Sosuke Ito, “Geometrical aspects of entropy production in stochastic thermodynamics based on wasserstein distance,” *Phys. Rev. Res.* **3**, 043093 (2021).
- [41] Tan Van Vu and Yoshihiko Hasegawa, “Geometrical bounds of the irreversibility in markovian systems,” *Phys. Rev. Lett.* **126**, 010601 (2021).
- [42] Tan Van Vu and Keiji Saito, “Thermodynamic unification of optimal transport: Thermodynamic uncertainty relation, minimum dissipation, and thermodynamic speed limits,” *Phys. Rev. X* **13**, 011013 (2023).
- [43] Erik Aurell, Carlos Mejía-Monasterio, and Paolo Muratore-Ginanneschi, “Optimal protocols and optimal transport in stochastic thermodynamics,” *Phys. Rev. Lett.* **106**, 250601 (2011).
- [44] Paolo Muratore-Ginanneschi, Carlos Mejía-Monasterio, and Luca Peliti, “Heat release by controlled continuous-time markov jump processes,” *J. Stat. Phys.* **150**, 181 (2013).
- [45] Paolo Muratore-Ginanneschi and Kay Schwieger, “How nanomechanical systems can minimize dissipation,” *Phys. Rev. E* **90**, 060102(R) (2014).
- [46] Giacomo Guarneri, Gabriel T. Landi, Stephen R. Clark, and John Goold, “Thermodynamics of precision in quantum nonequilibrium steady states,” *Phys. Rev. Research* **1**, 033021 (2019).
- [47] Kay Brandner and Keiji Saito, “Thermodynamic geometry of microscopic heat engines,” *Phys. Rev. Lett.* **124**, 040602 (2020).
- [48] Joshua Eglinton and Kay Brandner, “Geometric bounds on the power of adiabatic thermal machines,” *Phys. Rev. E* **105**, L052102 (2022).
- [49] Harry J. D. Miller, Matteo Scandi, Janet Anders, and Martí Perarnau-Llobet, “Work fluctuations in slow processes: Quantum signatures and optimal control,” *Phys. Rev. Lett.* **123**, 230603 (2019).
- [50] Paolo Abiuso and Martí Perarnau-Llobet, “Optimal cycles for low-dissipation heat engines,” *Phys. Rev. Lett.* **124**, 110606 (2020).
- [51] Harry J. D. Miller and Mohammad Mehboudi, “Geometry of work fluctuations versus efficiency in microscopic thermal machines,” *Phys. Rev. Lett.* **125**, 260602 (2020).
- [52] Paolo Abiuso, Harry JD Miller, Martí Perarnau-Llobet, and Matteo Scandi, “Geometric optimisation of quantum thermodynamic processes,” *Entropy* **22**, 1076 (2020).
- [53] Karel Proesmans, Jannik Ehrich, and John Bechhoefer, “Finite-time landauer principle,” *Phys. Rev. Lett.* **125**, 100602 (2020).
- [54] Jin-Fu Chen, C. P. Sun, and Hui Dong, “Extrapolating the thermodynamic length with finite-time measurements,” *Phys. Rev. E* **104**, 034117 (2021).
- [55] Pablo Terrén Alonso, Paolo Abiuso, Martí Perarnau-Llobet, and Liliana Arrachea, “Geometric optimization of nonequilibrium adiabatic thermal machines and implementation in a qubit system,” *PRX Quantum* **3**, 010326 (2022).
- [56] Adam G. Frim and Michael R. DeWeese, “Geometric bound on the efficiency of irreversible thermodynamic cycles,” *Phys. Rev. Lett.* **128**, 230601 (2022).
- [57] Adam G. Frim and Michael R. DeWeese, “Optimal finite-time brownian carnot engine,” *Phys. Rev. E* **105**, L052103 (2022).
- [58] Geng Li, Jin-Fu Chen, C. P. Sun, and Hui Dong, “Geodesic path for the minimal energy cost in shortcuts to isothermality,” *Phys. Rev. Lett.* **128**, 230603 (2022).
- [59] Matteo Scandi, David Barker, Sebastian Lehmann, Kimberly A. Dick, Ville F. Maisi, and Martí Perarnau-Llobet, “Minimally dissipative information erasure in a quantum dot via thermodynamic length,” *Phys. Rev. Lett.* **129**, 270601 (2022).
- [60] Paolo Abiuso, Viktor Holubec, Janet Anders, Zhuolin Ye, Federico Cerisola, and Martí Perarnau-Llobet, “Thermodynamics and optimal protocols of multidimensional quadratic brownian systems,” *J. Phys. Commun.* **6**, 063001 (2022).
- [61] Salambô Dago and Ludovic Bellon, “Dynamics of information erasure and extension of landauer’s bound to fast processes,” *Phys. Rev. Lett.* **128**, 070604 (2022).
- [62] Andre C. Barato and Udo Seifert, “Thermodynamic uncertainty relation for biomolecular processes,” *Phys. Rev. Lett.* **114**, 158101 (2015).
- [63] Todd R. Gingrich, Jordan M. Horowitz, Nikolay Perunov, and Jeremy L. England, “Dissipation bounds all steady-state current fluctuations,” *Phys. Rev. Lett.* **116**, 120601 (2016).
- [64] Todd R Gingrich, Grant M Rotskoff, and Jordan M Horowitz, “Inferring dissipation from current fluctuations,” *J. Phys. A* **50**, 184004 (2017).
- [65] Soham Pal, Sushant Saryal, Dvira Segal, T. S. Mahesh, and Bijay Kumar Agarwalla, “Experimental study of the thermodynamic uncertainty relation,” *Phys. Rev. Research* **2**, 022044(R) (2020).
- [66] Cheng Yang, Xinrui Wei, Jiteng Sheng, and Haibin Wu, “Phonon heat transport in cavity-mediated optomechanical nanoresonators,” *Nat. Commun.* **11**, 4656 (2020).
- [67] Patrick Pietzonka, Felix Ritort, and Udo Seifert, “Finite-time generalization of the thermodynamic uncertainty relation,” *Phys. Rev. E* **96**, 012101 (2017).
- [68] Kangqiao Liu, Zongping Gong, and Masahito Ueda, “Thermodynamic uncertainty relation for arbitrary initial states,” *Phys. Rev. Lett.* **125**, 140602 (2020).
- [69] Sushant Saryal and Bijay Kumar Agarwalla, “Bounds on fluctuations for finite-time quantum otto cycle,” *Phys. Rev. E* **103**, L060103 (2021).
- [70] Yoshihiko Hasegawa, “Quantum thermodynamic uncertainty relation for continuous measurement,” *Phys. Rev. Lett.* **125**, 050601 (2020).
- [71] Yoshihiko Hasegawa, “Thermodynamic uncertainty relation for general open quantum systems,” *Phys. Rev. Lett.* **126**, 010602 (2021).
- [72] Tan Van Vu and Keiji Saito, “Thermodynamics of precision in markovian open quantum dynamics,” *Phys. Rev. Lett.* **128**, 140602 (2022).

- [73] Katarzyna Macieszczak, Kay Brandner, and Juan P. Garrahan, “Unified thermodynamic uncertainty relations in linear response,” *Phys. Rev. Lett.* **121**, 130601 (2018).
- [74] Karel Proesmans and Jordan M Horowitz, “Hysteretic thermodynamic uncertainty relation for systems with broken time-reversal symmetry,” *J. Stat. Mech.: Theory Exp* **2019**, 054005.
- [75] Patrick P. Potts and Peter Samuelsson, “Thermodynamic uncertainty relations including measurement and feedback,” *Phys. Rev. E* **100**, 052137 (2019).
- [76] Massimiliano Esposito, Upendra Harbola, and Shaul Mukamel, “Nonequilibrium fluctuations, fluctuation theorems, and counting statistics in quantum systems,” *Rev. Mod. Phys.* **81**, 1665–1702 (2009).
- [77] Michele Campisi, Peter Hänggi, and Peter Talkner, “Colloquium: Quantum fluctuation relations: Foundations and applications,” *Rev. Mod. Phys.* **83**, 771–791 (2011).
- [78] Yoshihiko Hasegawa and Tan Van Vu, “Fluctuation theorem uncertainty relation,” *Phys. Rev. Lett.* **123**, 110602 (2019).
- [79] Jordan M Horowitz and Todd R Gingrich, “Thermodynamic uncertainty relations constrain non-equilibrium fluctuations,” *Nat. Phys.* **16**, 15–20 (2020).
- [80] Udo Seifert, “From stochastic thermodynamics to thermodynamic inference,” *Annu. Rev. Condens. Matter Phys.* **10**, 171–192 (2019).
- [81] Zhiyu Cao, Jie Su, Huijun Jiang, and Zhonghuai Hou, “Effective entropy production and thermodynamic uncertainty relation of active brownian particles,” *Phys. Fluids* **34**, 053310 (2022).
- [82] Zhiyu Cao and Zhonghuai Hou, “Improved estimation for energy dissipation in biochemical oscillations,” *J. Chem. Phys.* **157**, 025102 (2022).
- [83] Timur Koyuk, Udo Seifert, and Patrick Pietzonka, “A generalization of the thermodynamic uncertainty relation to periodically driven systems,” *J. Phys. A: Math. Theor* **52**, 02LT02 (2018).
- [84] Timur Koyuk and Udo Seifert, “Operationally accessible bounds on fluctuations and entropy production in periodically driven systems,” *Phys. Rev. Lett.* **122**, 230601 (2019).
- [85] Timur Koyuk and Udo Seifert, “Thermodynamic uncertainty relation for time-dependent driving,” *Phys. Rev. Lett.* **125**, 260604 (2020).
- [86] Christian Maes, “Frenesy: Time-symmetric dynamical activity in nonequilibria,” *Phys. Rep.* **850**, 1–33 (2020).
- [87] For details, see the supplement, which includes Ref. [19, 36, 47, 64, 68, 85, 89].
- [88] Y. Aharonov and J. Anandan, “Phase change during a cyclic quantum evolution,” *Phys. Rev. Lett.* **58**, 1593–1596 (1987).
- [89] Andreas Dechant and Shin-ichi Sasa, “Fluctuation–response inequality out of equilibrium,” *Proc. Natl. Acad. Sci. U.S.A.* **117**, 6430 (2020).
- [90] Jincheng Lu, Zi Wang, Jiebin Peng, Chen Wang, Jian-Hua Jiang, and Jie Ren, “Geometric thermodynamic uncertainty relation in a periodically driven thermoelectric heat engine,” *Phys. Rev. B* **105**, 115428 (2022).
- [91] R Dean Astumian and Peter Hänggi, “Brownian motors,” *Phys. Today* **55**, 33–39 (2002).
- [92] Ronnie Kosloff and Amikam Levy, “Quantum heat engines and refrigerators: Continuous devices,” *Annu. Rev. Phys. Chem.* **65**, 365–393 (2014).
- [93] V. Y. Chernyak and N. A. Sinitsyn, “Pumping restriction theorem for stochastic networks,” *Phys. Rev. Lett.* **101**, 160601 (2008).
- [94] Kay Brandner, Michael Bauer, and Udo Seifert, “Universal coherence-induced power losses of quantum heat engines in linear response,” *Phys. Rev. Lett.* **119**, 170602 (2017).
- [95] Krzysztof Ptaszyński, “Coherence-enhanced constancy of a quantum thermoelectric generator,” *Phys. Rev. B* **98**, 085425 (2018).
- [96] Patrice A. Camati, Jonas F. G. Santos, and Roberto M. Serra, “Coherence effects in the performance of the quantum otto heat engine,” *Phys. Rev. A* **99**, 062103 (2019).
- [97] Gernot Schaller, *Open quantum systems far from equilibrium*, Vol. 881 (Springer, 2014).
- [98] Chen Wang, Hua Chen, and Jie-Qiao Liao, “Nonequilibrium thermal transport and photon squeezing in a quadratic qubit-resonator system,” *Phys. Rev. A* **104**, 033701 (2021).

Supplement: Thermodynamic Geometry of Nonequilibrium Fluctuations in Cyclically Driven Transport

Zi Wang and Jie Ren*

Center for Phononics and Thermal Energy Science, China-EU Joint Lab on Nanophononics, Shanghai Key Laboratory of Special Artificial Microstructure Materials and Technology, School of Physics Science and Engineering, Tongji University, Shanghai 200092, China

(Dated: March 15, 2024)

In Sec. I, we provide the details of the full counting statistics (FCS) in the Markovian dynamics. In Sec. II, we present the derivation of our geometric separation of FCS in a periodically driven thermal device and show its manifestation as a metric term. In Sec. III, the formulae for average currents are derived based on our geometric theory on FCS. In Sec. IV, we illustrate our geometric non-adiabatic control principle. In Sec. V, we derive our geometric thermodynamic uncertainty relation (TUR) and its implication on the fluctuation of entropy production. Finally, the details for the two models exemplified in the main text are provided in Sec. VI.

I. GENERAL MARKOVIAN DYNAMICS

In this section, we discuss the basic theory for the generating function of a fluctuating current.

We consider a periodically driven discrete Markovian system coupled to several reservoirs. Its probability distribution p_i is labeled by i ($1 \leq i \leq N$), with N being the overall number of states. The rate along the transition $j \rightarrow i$ induced by the ν -th reservoir is k_{ij}^ν ($i \neq j$), whose time-dependence is kept implicit for clarity. As demanded by the thermodynamic consistency, we assume the local detailed balance condition $k_{ij}^\nu/k_{ji}^\nu = e^{\beta_\nu(E_j - E_i)}$, with $\beta_\nu := 1/T_\nu$ being the inverse temperature of the ν -th reservoir (Boltzmann constant is set to 1) and E_i the energy level of the system. The master equation of p_i is $\partial_t |p(t)\rangle = \hat{L} |p(t)\rangle$, with $L_{ij} := \sum_\nu (k_{ij}^\nu - \delta_{ij} \sum_{j \neq i} k_{ji}^\nu)$ preserving probability by $\sum_i L_{ij} = 0$.

The transition k_{ij}^ν is associated with an accumulation of exchange current $\Delta Q = d_{ij}^\nu$ ($d_{ij}^\nu = -d_{ji}^\nu$). The accumulated current Q can be particle number, energy, entropy, work, and so on, which in the special case of $d_{ij}^\nu = \ln(k_{ij}^\nu/k_{ji}^\nu)$ corresponds to the reservoir entropy production Σ . To consider the fluctuation of this current, we take advantage of the full counting statistics formalism. We twist the operator \hat{L} to \hat{L}_χ , with $L_{\chi,ij} = \sum_\nu k_{ij}^\nu e^{\chi d_{ij}^\nu}$ for $i \neq j$ and $L_{\chi,ii} = L_{ii}$. Here, χ is the counting field of Q . Taking the derivative of the cumulant generating function (CGF)

$$\mathcal{G} = \ln \mathcal{Z} = \ln \langle 1 | p_\chi(t) \rangle \quad (\text{S1})$$

with respect to χ yields the n -th cumulant of the accumulated current Q during $[0, t]$

$$\langle Q^n \rangle_c = \frac{\partial^n \mathcal{G}}{\partial \chi^n} \Big|_{\chi=0}. \quad (\text{S2})$$

Here, $|p_\chi(t)\rangle$ is generated by the equation of motion $\partial_t |p_\chi(t)\rangle = \hat{L}_\chi |p_\chi(t)\rangle$ and $\langle 1 |$ is a vector with all elements being 1. We note that the characteristic function \mathcal{Z} satisfies $\mathcal{Z}|_{\chi=0} = 1$ due to the probability normalization condition $\langle 1 | p_\chi \rangle|_{\chi=0} = 1$. As a result, the CGF has the property $\mathcal{G}|_{\chi=0} = 0$.

This is equivalent to the path integral formalism. By assigning the weight to a trajectory $\omega = x(t)$ ($0 \leq t \leq \tau$)

$$P[\omega] = p(x_0) e^{-\int_0^\tau dt \sum_{i \neq j, \nu} [\delta_{x(t), i} k_{ji}^\nu(t) - \dot{m}_{ji}^\nu \ln k_{ji}^\nu(t)]}, \quad (\text{S3})$$

with $p(x_0)$ being the initial distribution at $t = 0$ and m_{ij}^ν counting the accumulated number of transition k_{ij}^ν , the CGF is also expressed as

$$\mathcal{G} = \ln \int d\omega p(x_0) e^{-\int_0^\tau dt \sum_{i \neq j, \nu} [\delta_{x(t), i} k_{ji}^\nu(t) - \dot{m}_{ji}^\nu (\chi d_{ji}^\nu(t) + \ln k_{ji}^\nu(t))]} \quad (\text{S4})$$

The overdamped Brownian dynamics can be taken as a specific limit case of this discrete transition dynamics [1].

II. DYNAMIC AND GEOMETRIC COMPONENTS OF THE CGF

Here, we derive the general geometric components of the current fluctuation and its metric component.

We start from the equation of motion $\partial_t |p_\chi(t)\rangle = \hat{L}_\chi(\mathbf{\Lambda}(t)) |p_\chi(t)\rangle$, where $\mathbf{\Lambda}(t)$ is the periodically driven parameter vector with period τ_p . Suppose that \hat{L}_χ can be diagonalized $\hat{L}_\chi = \sum_n E_n |r_n\rangle \langle l_n|$, with E_n , $|r_n\rangle$ and $\langle l_n|$ being respectively the eigenvalue, right- and left-eigenvectors satisfying $\hat{L}_\chi |r_n\rangle = E_n |r_n\rangle$ and $\langle l_n| \hat{L}_\chi = E_n \langle l_n|$ and the orthonormal condition $\langle l_m | r_n \rangle = \delta_{m,n}$. The eigenvectors $|r_n\rangle$ and $\langle l_n|$ and the eigenvalues E_n are all functions of the counting parameter χ . $n = 0$ corresponds to the steady state. We also note that by taking $\chi = 0$, the twisted operator \hat{L}_χ reduces to \hat{L} , $|r_0\rangle$ to the steady state distribution $|\pi\rangle$ and $\langle l_0|$ to the one-vector $\langle 1|$. After a large number of periods, the system enters its cyclic state. According to the Floquet theorem, the system state is of the form

$$|p_\chi(t)\rangle = e^{\mathcal{G}(t)} |\phi(t)\rangle, \quad (\text{S5})$$

where $|\phi(t + \tau_p)\rangle = |\phi(t)\rangle$ is a cyclic state and $|p_\chi(t)\rangle$ only accumulates an CGF phase $\mathcal{G}(\tau_p)$ during one driving period. Inserting this ansatz into the equation of motion, the dynamics of $|\phi(t)\rangle$ is governed by

$$(\hat{L}_\chi - \partial_t) |\phi(t)\rangle = (\partial_t \mathcal{G}(t)) |\phi(t)\rangle. \quad (\text{S6})$$

* Corresponding Email: Xonics@tongji.edu.cn

The operator ∂_t can be seen as a perturbation to the steady state. In the absence of ∂_t , Eq. (S6) is solved by the state $|\phi(t)\rangle = |r_0\rangle$ and the equation for CGF

$$\partial_t \mathcal{G}_{\text{dyn}}(t) = E_0(t), \quad (\text{S7})$$

which corresponds to the dynamic-phase-like contribution

$$\mathcal{G}_{\text{dyn}}(\tau_p) = \int_0^{\tau_p} dt E_0(t). \quad (\text{S8})$$

Denoting the deviation of $\mathcal{G}(t)$ from $\mathcal{G}_{\text{dyn}}(t)$ as $\mathcal{G}_{\text{geo}}(t) = \mathcal{G}(t) - \mathcal{G}_{\text{dyn}}(t)$, which is later shown to be a general geometric phase like contribution applicable to arbitrary driving frequency, we can write Eq. (S6) as

$$[\hat{L}_\chi - E_0(t)] |\phi(t)\rangle = [\partial_t + \partial_t \mathcal{G}_{\text{geo}}(t)] |\phi(t)\rangle. \quad (\text{S9})$$

Taking the inner product of both sides with $\langle l_0|$, the left hand side is zero. Thus, the right hand side is orthogonal to $|r_0\rangle$ and we derive the equation for \mathcal{G}_{geo} as $(\partial_t \mathcal{G}_{\text{geo}}) \langle l_0|\phi\rangle = -\langle l_0|\partial_t\phi\rangle$. This leaves a gauge degree of freedom for $|\phi\rangle$. If we make the gauge transform $|\phi\rangle \rightarrow e^{\alpha(t)} |\phi\rangle$, $\partial_t \mathcal{G}_{\text{geo}}$ is changed to $\partial_t \mathcal{G}_{\text{geo}} + \partial_t \alpha(t)$, ensuring the gauge-invariance of $\mathcal{G}_{\text{geo}}(\tau_p)$ since $\int_0^{\tau_p} dt \partial_t \alpha = 0$.

We can fix the gauge of $|\phi(t)\rangle$ by requiring its form

$$|\phi\rangle = |r_0\rangle + |\phi_\perp\rangle, \quad (\text{S10})$$

where $\langle l_0|\phi_\perp\rangle = 0$. Substituting this expression into Eq. (S9), we obtain

$$(\hat{L}_\chi - E_0) |\phi_\perp\rangle = |\partial_t r_0\rangle + |\partial_t \phi_\perp\rangle + (\partial_t \mathcal{G}_{\text{geo}})(|r_0\rangle + |\phi_\perp\rangle), \quad (\text{S11})$$

the inner product of which and $\langle l_0|$ provides an equation for \mathcal{G}_{geo} :

$$\partial_t \mathcal{G}_{\text{geo}} = -\langle l_0|\partial_t r_0\rangle - \langle l_0|\partial_t \phi_\perp\rangle := \partial_t \mathcal{G}_{\text{curv}} + \partial_t \mathcal{G}_{\text{metr}}, \quad (\text{S12})$$

where we identify the curvature term and the metric term. They describe respectively the adiabatic and nonadiabatic effect of the driving. Through a whole period, the curvature term is

$$\mathcal{G}_{\text{curv}}(\tau_p) = \oint_{\partial\Omega} d\Lambda_\mu A_\mu := -\oint_{\partial\Omega} d\Lambda_\mu \langle l_0|\partial_\mu r_0\rangle, \quad (\text{S13})$$

where we define the geometric connection $A_\mu = -\langle l_0|\partial_\mu r_0\rangle$. Using the Stokes formula, this is equivalent to

$$\mathcal{G}_{\text{curv}}(\tau_p) = \int_\Omega dS_{\mu\nu} F_{\mu\nu}, \quad (\text{S14})$$

in terms of the geometric curvature $F_{\mu\nu} := \partial_\mu A_\nu - \partial_\nu A_\mu = -\langle \partial_\mu l_0|\partial_\nu r_0\rangle + \langle \partial_\nu l_0|\partial_\mu r_0\rangle$.

Now we focus on the metric term $\mathcal{G}_{\text{metr}}$. We first note

$$\begin{aligned} \mathcal{G}_{\text{metr}}(\tau_p) &= -\int_0^{\tau_p} dt \langle l_0|\partial_t \phi_\perp\rangle \\ &= \int_0^{\tau_p} dt \langle \partial_t l_0|\phi_\perp\rangle. \end{aligned} \quad (\text{S15})$$

Since Eq. (S11) can be formally solved as

$$\begin{aligned} |\phi_\perp\rangle &= (\hat{L}_\chi - E_0)^+ |\partial_t \phi\rangle + (\partial_t \mathcal{G}_{\text{geo}})(\hat{L}_\chi - E_0)^+ |\phi_\perp\rangle \\ &= (\hat{L}_\chi - E_0)^+ |\partial_t \phi\rangle - (\hat{L}_\chi - E_0)^+ |\phi\rangle \langle l_0|\partial_t \phi\rangle, \end{aligned} \quad (\text{S16})$$

with the pseudo-inverse being $(\hat{L}_\chi - E_0)^+ := \sum_{n \neq 0} \frac{1}{E_n - E_0} |r_n\rangle \langle l_n|$, we derive the metric expression

$$\mathcal{G}_{\text{metr}}(\tau_p) = \int_0^{\tau_p} dt g_{tt} := \int_0^{\tau_p} dt \langle \partial_t l_0|\hat{G}|\partial_t \phi\rangle. \quad (\text{S17})$$

Here, we define the metric tensor as

$$\hat{G} = (\hat{L}_\chi - E_0)^+ - (\hat{L}_\chi - E_0)^+ |\phi\rangle \langle l_0|. \quad (\text{S18})$$

This metric structure also endows a pseudo-Riemannian manifold in the driven parameter space. In terms of this, $\mathcal{G}_{\text{metr}}$ can be written as

$$\mathcal{G}_{\text{metr}} = \int_0^{\tau_p} g_{\mu\nu} \dot{\Lambda}_\mu \dot{\Lambda}_\nu dt, \quad (\text{S19})$$

$$\text{with } g_{\mu\nu} := \frac{1}{2} \left[\langle \partial_\mu l_0|\hat{G}|\partial_\nu \phi\rangle + \langle \partial_\nu l_0|\hat{G}|\partial_\mu \phi\rangle \right].$$

In contrast to the Riemannian manifold, the metric $[g_{\mu\nu}]$ is not necessarily positive-definite. This sacrifice makes our formalism applicable to the whole fluctuation properties of an arbitrary current.

When the near-adiabatic regime is concerned, the Floquet state $|\phi\rangle$ can be approximated, to the leading order, as $|r_0\rangle$. This provides the nonadiabatic metric structure

$$\begin{aligned} g_{\mu\nu} &= \frac{1}{2} \left[\langle \partial_\mu l_0|\hat{G}|\partial_\nu r_0\rangle + \langle \partial_\nu l_0|\hat{G}|\partial_\mu r_0\rangle \right] \\ &= \sum_{n \neq 0} \frac{\langle \partial_\mu l_0|r_n\rangle \langle l_n|\partial_\nu r_0\rangle + \langle \partial_\nu l_0|r_n\rangle \langle l_n|\partial_\mu r_0\rangle}{2(E_n - E_0)}, \end{aligned} \quad (\text{S20})$$

which describes the leading finite-time effect in the near-adiabatic regime. Away from this regime, the exact $|\phi\rangle$ can be obtained by using the Dyson-series-like self-consistent equation Eq. (S16) with iteration.

Therefore, as a summary the CGF has the decomposition:

$$\mathcal{G} = \mathcal{G}_{\text{dyn}} + \mathcal{G}_{\text{geo}} = \mathcal{G}_{\text{dyn}} + \mathcal{G}_{\text{curv}} + \mathcal{G}_{\text{metr}}. \quad (\text{S21})$$

We note that the above formalism is applicable to arbitrary time antisymmetric current in general nonequilibrium conditions. This provides the basis for analyzing the fluctuation properties of a finite-time cyclically driven thermal device.

III. AVERAGE GEOMETRIC CURRENTS

Here, we derive the average current based on our FCS theory.

In this section, $|p\rangle$ and \hat{L} without the subscript χ means $|p_\chi\rangle|_{\chi=0}$ and $\hat{L}_\chi|_{\chi=0}$.

First, we consider the total accumulated current and show that the mean value $\langle Q \rangle = \partial_\chi \mathcal{G}(\tau_p)|_{\chi=0}$ is also expressed as

$$\langle Q \rangle = \int_0^{\tau_p} dt \langle 1 | \hat{J}(t) | p(t) \rangle, \quad (\text{S22})$$

where the current density operator is given by $\hat{J} = \partial_\chi \hat{L}_\chi|_{\chi=0}$. Eq. (S22) is important in studying both the average current in stochastic systems and the current in deterministic systems. Defining the propagator for the twisted dynamics $\partial_t |p_\chi(t)\rangle = \hat{L}_\chi |p_\chi(t)\rangle$ as

$$\hat{U}_\chi(t_2, t_1) = \mathcal{T} e^{\int_{t_1}^{t_2} dt \hat{L}_\chi(t)}, \quad (\text{S23})$$

in terms of the time-ordering operator \mathcal{T} , we note that the Floquet state Eq. (S5) is the eigenstate of $\hat{U}_\chi(\tau_p, 0)$

$$\hat{U}_\chi(\tau_p, 0) |p_\chi(0)\rangle = e^{\mathcal{G}(\tau_p)} |p_\chi(0)\rangle. \quad (\text{S24})$$

We differentiate both side with respect to χ , set $\chi = 0$ and take the inner product with $\langle 1 |$. The left hand side is

$$\begin{aligned} & \langle 1 | [\partial_\chi \hat{U}_\chi(\tau_p, 0)] | p_\chi(0) \rangle |_{\chi=0} + \langle 1 | \hat{U}_\chi(\tau_p, 0) | \partial_\chi p_\chi(0) \rangle |_{\chi=0} \\ &= \int_0^{\tau_p} dt \langle 1 | \hat{J} | p(t) \rangle + \langle 1 | \partial_\chi p_\chi(0) \rangle |_{\chi=0}, \end{aligned} \quad (\text{S25})$$

using $\partial_\chi \hat{U}_\chi(\tau_p, 0) = \int_0^{\tau_p} dt \hat{U}_\chi(\tau_p, t) [\partial_\chi \hat{L}_\chi(t)] \hat{U}_\chi(t, 0)$ and $\langle 1 | \hat{U}_\chi |_{\chi=0} = \langle 1 |$. The right hand side is

$$\begin{aligned} & [\partial_\chi \mathcal{G}(\tau_p)] e^{\mathcal{G}(\tau_p)} \langle 1 | p_\chi(0) \rangle |_{\chi=0} + e^{\mathcal{G}(\tau_p)} \langle 1 | \partial_\chi p_\chi(0) \rangle |_{\chi=0} \\ &= \langle Q \rangle + \langle 1 | \partial_\chi p_\chi(0) \rangle |_{\chi=0}, \end{aligned} \quad (\text{S26})$$

using $\mathcal{G}(\tau_p)|_{\chi=0} = 0$, the definition $\langle Q \rangle := \partial_\chi \mathcal{G}(\tau_p)|_{\chi=0}$ and the normalization condition $\langle 1 | p_\chi(0) \rangle |_{\chi=0} = \langle 1 | p(0) \rangle = 1$. Combining these results, we arrive at the identity for average total accumulated current Eq. (S22).

Second, we consider the dynamic current component. To prove

$$\langle Q_{\text{dyn}} \rangle := \partial_\chi \mathcal{G}_{\text{dyn}}(\tau_p)|_{\chi=0} = \int_0^{\tau_p} dt \langle 1 | \hat{J} | \pi(t) \rangle, \quad (\text{S27})$$

with $|\pi\rangle = |r_0\rangle|_{\chi=0}$ being the instantaneous steady state, we start from the eigenvalue equation

$$\hat{L}_\chi |r_0\rangle = E_0 |r_0\rangle. \quad (\text{S28})$$

Calculating the derivative at $\chi = 0$ and taking inner product with $\langle 1 |$, the left hand side is $\langle 1 | \hat{J} | \pi \rangle + \langle 1 | \hat{L}_\chi | \partial_\chi r_0 \rangle |_{\chi=0} = \langle 1 | \hat{J} | \pi \rangle$ using the property $\langle 1 | \hat{L} = 0$, while the right hand side is $\partial_\chi E_0|_{\chi=0}$ since $|\pi\rangle$ is normalized and $E_0|_{\chi=0} = 0$. Therefore, we have the result $\partial_\chi E_0|_{\chi=0} = \langle 1 | \hat{J}(t) | \pi(t) \rangle$ and consequently Eq. (S27).

Thirdly, we consider the general geometric current. For the cyclic state $|\phi(t)\rangle$, we note that the corresponding average current density $-\partial_\chi \langle l_0 | \partial_t \phi \rangle |_{\chi=0}$ is identical

to $-\langle \partial_\chi l_0 | \partial_t \phi \rangle |_{\chi=0}$ up to a complete differential term $-\langle l_0 | \partial_\chi \partial_t \phi \rangle |_{\chi=0} = -\partial_t \langle 1 | \partial_\chi \phi \rangle |_{\chi=0}$, for any cyclic $|\phi\rangle$. This complete differential term makes no contribution when integrating over a whole period. By further showing the identity

$$\langle \partial_\chi l_0 | \hat{L} |_{\chi=0} + \langle 1 | \hat{J} = \langle 1 | (\partial_\chi E_0) |_{\chi=0}, \quad (\text{S29})$$

and therefore

$$\langle \partial_\chi l_0 |_{\chi=0} = \langle \partial_\chi l_0 | r_0 \rangle |_{\chi=0} \langle 1 | - \langle 1 | \hat{J} \hat{L}^+, \quad (\text{S30})$$

where \hat{L}^+ is the pseudo-inverse of \hat{L} , we prove that our formulation in terms of CGF provides the expression for average accumulated geometric current

$$\begin{aligned} \langle Q_{\text{geo}} \rangle &:= \partial_\chi \mathcal{G}_{\text{geo}}|_{\chi=0} = - \int_0^{\tau_p} dt \partial_\chi \langle l_0 | \partial_t \phi \rangle |_{\chi=0} \\ &= - \int_0^{\tau_p} dt \langle \partial_\chi l_0 | \partial_t \phi \rangle |_{\chi=0} \\ &= - \int_0^{\tau_p} dt \left[\langle \partial_\chi l_0 | r_0 \rangle \langle 1 | \partial_t \phi \rangle - \langle 1 | \hat{J} \hat{L}^+ | \partial_t \phi \rangle \right] |_{\chi=0} \\ &= \int_0^{\tau_p} dt \langle 1 | \hat{J} \hat{L}^+ | \partial_t p(t) \rangle. \end{aligned} \quad (\text{S31})$$

The fourth equality is due to the constant normalization condition $\partial_t \langle 1 | \phi \rangle |_{\chi=0} = 0$. This expression of $\langle Q_{\text{geo}} \rangle$ simplifies to the adiabatic geometric current

$$\begin{aligned} \langle Q_{\text{curv}} \rangle &= \oint_{\partial\Omega} d\Lambda_\mu \langle 1 | \hat{J} \hat{L}^+ | \partial_\mu \pi(t) \rangle \\ &= \int_\Omega d\Lambda_\mu d\Lambda_\nu [\langle 1 | \partial_\mu (\hat{J} \hat{L}^+) | \partial_\nu \pi \rangle - \langle 1 | \partial_\nu (\hat{J} \hat{L}^+) | \partial_\mu \pi \rangle], \end{aligned} \quad (\text{S32})$$

and the nonadiabatic geometric current

$$\begin{aligned} \langle Q_{\text{metr}} \rangle &= \int_0^{\tau_p} dt \langle 1 | \hat{J} \hat{L}^+ | \partial_t \phi_\perp \rangle |_{\chi=0} \\ &= \int_0^{\tau_p} dt \langle 1 | \hat{J} \hat{L}^+ \partial_t [(\hat{L}_\chi - E_0)^+ | \partial_t \phi \rangle] |_{\chi=0} \\ &= \int_0^{\tau_p} dt \langle 1 | \hat{J} \hat{L}^+ \partial_t [(\hat{L}_\chi - E_0)^+ | \phi \rangle \langle l_0 | \partial_t \phi \rangle] |_{\chi=0} \\ &= \int_0^{\tau_p} dt \langle 1 | \hat{J} \hat{L}^+ \partial_t [\hat{L}^+ | \partial_t p \rangle] \\ &= \int_0^{\tau_p} dt \dot{\Lambda}_\mu \dot{\Lambda}_\nu \frac{1}{2} \left[\langle 1 | \hat{J} \hat{L}^+ \partial_\mu (\hat{L}^+ | \partial_\nu p \rangle) + (\mu \leftrightarrow \nu) \right] \\ &:= \int_0^{\tau_p} dt \dot{\Lambda}_\mu \dot{\Lambda}_\nu g_{\mu\nu}^Q. \end{aligned} \quad (\text{S33})$$

Here, $g_{\mu\nu}^Q$ is the metric related to the average current Q .

Correspondingly, the near-adiabatic metric for average Q is obtained by replacing $|p\rangle$ in Eq. (S33) by $|\pi\rangle$:

$$g_{\mu\nu}^Q = \frac{1}{2} \left[\langle 1 | \hat{J} \hat{L}^+ \partial_\mu (\hat{L}^+ | \partial_\nu \pi \rangle) + (\mu \leftrightarrow \nu) \right]. \quad (\text{S34})$$

Therefore, we have shown the decomposition for the average currents

$$\langle Q \rangle = \langle Q_{\text{dyn}} \rangle + \langle Q_{\text{geo}} \rangle = \langle Q_{\text{dyn}} \rangle + \langle Q_{\text{curv}} \rangle + \langle Q_{\text{metr}} \rangle. \quad (\text{S35})$$

We note here that the above derived average current components are part of our general geometric formulation. Our CGF theory is indispensable in analyzing the fluctuations of finite-time periodically driven systems.

IV. NON-ADIABATIC CONTROL OVER CURRENT PUMP

Here, we discuss the non-adiabatic geometric control over current pump effect.

The metric $\mathfrak{g}_{\mu\nu}^Q$ for an arbitrary current Q is not guaranteed to be positive definite. It can have both positive and negative eigenvalues. If we pass through the positive (negative) eigenvector directions, the non-adiabatic geometric current is along its positive (negative) direction. Between the negative and positive eigenvectors, there must exist a direction where $\mathfrak{g}_{\mu\nu} \hat{\Lambda}_\mu \hat{\Lambda}_\nu = 0$ is satisfied. If we design our driving protocol to be along these zero-vector directions, we can eliminate the non-adiabatic pump effect. This constructs a non-adiabatic geometric control over the current pump effect.

Here, we demonstrate this control principle with a two-level-system (TLS) model in Fig. S1. It is composed of a TLS of energy difference ω and is coupled to two reservoirs of the same temperature T . We drive the parameter $\Lambda := (\omega, T)^T$. By counting the heat current Q from the left reservoir into the TLS, we obtain the twisted master equation operator

$$\hat{L}_\chi = \begin{pmatrix} -2n & (1+n)(e^{-\chi\omega} + 1) \\ n(e^{\chi\omega} + 1) & -2(1+n) \end{pmatrix}, \quad (\text{S36})$$

where χ is the counting parameter and $n = 1/(e^{\omega/T} - 1)$ is the Bose-Einstein distribution. Using Eq. (S20), we obtain the metric in parameter space as

$$\mathfrak{g}^Q = \partial_\chi \mathfrak{g}|_{\chi=0} = \frac{1}{4T^2} \text{csch}^3\left(\frac{\omega}{T}\right) \sinh^4\left(\frac{\omega}{2T}\right) \begin{pmatrix} -2T & \omega \\ \omega & 0 \end{pmatrix}. \quad (\text{S37})$$

It indeed has both positive and negative eigenvalues and we illustrate its corresponding zero-vector direction field in Fig. S1. This non-adiabatic control principle can also be used to regulate other types of generic currents and their cumulants.

V. DERIVATION OF GEOMETRIC TURS

The geometric TUR for cyclically driven thermal device is derived in this section.

We set the counting parameter $\chi = 0$ in this proof. Starting from $\partial_t |p(t)\rangle = \hat{L}(t) |p(t)\rangle$, we obtain a self-consistent equation for $|\delta(t)\rangle = |p(t)\rangle - |\pi(t)\rangle$:

$$|\delta(t)\rangle = \hat{L}^+ |\partial_t \pi(t)\rangle + \hat{L}^+ |\partial_t \delta\rangle, \quad (\text{S38})$$

where $|\pi\rangle$ is the instantaneous steady state satisfying $\hat{L}(t) |\pi(t)\rangle = 0$ and \hat{L}^+ is the pseudo-inverse of \hat{L} . \hat{L}^+ is

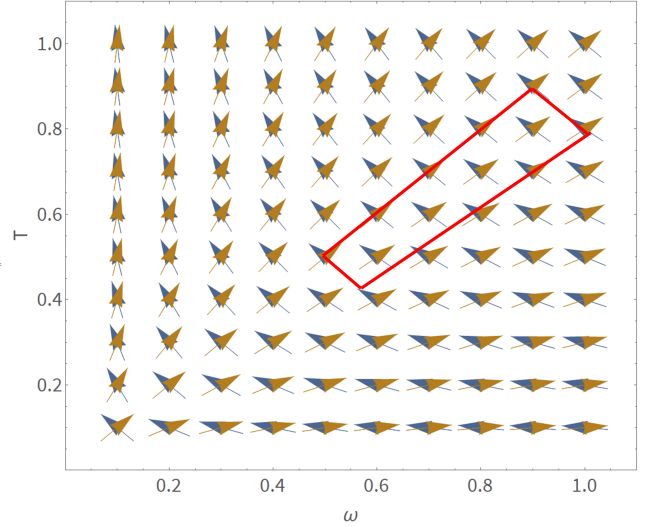


FIG. S1. **The non-adiabatic geometric control over current pump.** In the parameter space composed of system energy level difference ω and the bath temperature T , the arrows illustrates the direction of zero non-adiabatic directions, along which $\mathfrak{g}_{\mu\nu}^Q \hat{\Lambda}_\mu \hat{\Lambda}_\nu = 0$ is satisfied. By designing contours along this zero direction field, as shown in the red curve, we can eliminate the non-adiabatic effect of current pump effect.

defined by $\hat{L}^+ \hat{L} = \hat{L} \hat{L}^+ = \hat{I} - |\pi\rangle \langle 1|$, with \hat{I} being the identity operator and $\langle 1|$ the one-vector. By recurrently substituting, it is obvious to obtain the adiabatic and nonadiabatic corrections to the distribution $|p\rangle = |\pi\rangle + |p_{\text{curv}}\rangle + |p_{\text{metr}}\rangle$ respectively, where $|p_{\text{curv}}\rangle = \hat{L}^+ |\partial_t \pi(t)\rangle$ and $|p_{\text{metr}}\rangle = \hat{L}^+ \partial_t (\hat{L}^+ |\partial_t \pi(t)\rangle)$.

The current operator \hat{J} is defined by $J_{ij} = \sum_\mu k_{ij}^\mu d_{ij}^\mu$ in terms of the transition rates k_{ij}^μ and the antisymmetric tensor $d_{ij}^\mu = -d_{ji}^\mu$. The component d_{ij}^μ is the stochastic current accompanying the transition $j \rightarrow i$ induced by the reservoir μ . In these notations, the adiabatic and nonadiabatic geometric currents are

$$\begin{aligned} \langle Q_{\text{curv}} \rangle &= \int_\Omega dS_{\mu\nu} F_{\mu\nu}^Q, \\ \langle Q_{\text{metr}} \rangle &= \int_0^{\tau_p} dt \dot{\Lambda}_\mu \dot{\Lambda}_\nu \mathfrak{g}_{\mu\nu}^Q, \end{aligned} \quad (\text{S39})$$

where $F_{\mu\nu}^Q = \langle 1 | \partial_\mu (\hat{J} \hat{L}^+) | \partial_\nu \pi \rangle - \langle 1 | \partial_\nu (\hat{J} \hat{L}^+) | \partial_\mu \pi \rangle$, $\mathfrak{g}_{\mu\nu}^Q = \frac{1}{2} \left[\langle 1 | \hat{J} \hat{L}^+ \partial_\mu (\hat{L}^+ | \partial_\nu \pi \rangle) + (\mu \leftrightarrow \nu) \right]$. We note here that these expression for the average current can also be derived from Eq. (S14) and Eq. (S20) by taking derivative to χ and then setting $\chi \rightarrow 0$, as shown in Sec. III.

Now, let us start our proof of Geometric TURs from the fluctuation-response inequality [2], which is equivalent to the classical Cramer-Rao bound in the linear response regime. Similar method has been adopted by [3, 4] in deriving their TURs. Our method here is similar to those used by Ref. [2] in proving their generalized TURs. We consider a virtual perturbation on the transition rates, with θ being its perturbation

strength. Considering the Kullback-Leibler (KL) divergence of the perturbed and unperturbed trajectory weight to the order of θ^2 , one can write

$$\begin{aligned} D_{\text{KL}} &= \int d\omega P_\theta(\omega) \ln\left(\frac{P_\theta(\omega)}{P_0(\omega)}\right) \\ &= \frac{\theta^2}{2} \int d\omega P_0(\omega) [\partial_\theta \ln P_\theta(\omega)|_{\theta \rightarrow 0}]^2 + \mathcal{O}(\theta^3) \\ &= -\frac{\theta^2}{2} \int d\omega P_0(\omega) [\partial_\theta^2 \ln P_\theta(\omega)|_{\theta \rightarrow 0}] + \mathcal{O}(\theta^3) \\ &= -\frac{\theta^2}{2} \langle \partial_\theta^2 \ln P_\theta|_{\theta \rightarrow 0} \rangle_0 + \mathcal{O}(\theta^3). \end{aligned} \quad (\text{S40})$$

For the discrete Markovian systems, the weight for the trajectory $\omega = x(t)$ is given by [3]

$$P_\theta(\omega) = p(x_0) e^{-\int_0^{\tau_p} dt \sum_{i \neq j; \mu} [\delta_{x(t), i} k_{ji}^\mu(\theta, t) - \tau m_{ji}^\mu \ln k_{ji}^\mu(\theta, t)]}, \quad (\text{S41})$$

where $p(x_0)$ is the initial condition and m_{ij}^μ is the accumulated number of transitions. The basic average quantities are given by $\langle \delta_{x(t), i} \rangle_\theta = p_i(\theta, t)$ and $\langle \dot{m}_{ij}^\mu \rangle_\theta = p_j(\theta, t) k_{ij}^\mu(\theta, t)$. We choose the form of the virtual perturbation to be $k_{ij}^\mu(\theta, t) = k_{ij}^\mu e^{\theta \alpha_{ij}^\mu(t)}$. By showing $\partial_\theta^2 \ln P_\theta|_{\theta \rightarrow 0} = -\sum_{i \neq j; \mu} \int_0^{\tau_p} dt \delta_{x(t), i} k_{ji}^\mu (\alpha_{ji}^\mu)^2$, we express the KL divergence as

$$\begin{aligned} D_{\text{KL}} &\approx -\frac{\theta^2}{2} \langle \partial_\theta^2 \ln P_\theta|_{\theta \rightarrow 0} \rangle_0 \\ &= \frac{\theta^2}{2} \sum_{i \neq j; \mu} \int_0^{\tau_p} dt \langle \delta_{x(t), i} \rangle_0 k_{ji}^\mu(t) [\alpha_{ji}^\mu(t)]^2 \\ &= \frac{\theta^2}{2} \sum_{i \neq j; \mu} \int_0^{\tau_p} dt p_i(t) k_{ji}^\mu(t) [\alpha_{ji}^\mu(t)]^2 \\ &= \frac{\theta^2}{2} \sum_{i > j; \mu} \int_0^{\tau_p} dt \frac{[j_{ji}^\mu(t)]^2}{t_{ji}^\mu(t)}. \end{aligned} \quad (\text{S42})$$

Here we select $\alpha_{ij}^\mu = j_{ij}^\mu / t_{ij}^\mu$ in the last line, where we define the detailed current $j_{ij}^\mu = p_j k_{ij}^\mu - p_i k_{ji}^\mu$ and the activity $t_{ij}^\mu = p_j k_{ij}^\mu + p_i k_{ji}^\mu$. By using the log-sum inequality $\frac{2(b-a)^2}{a+b} \leq (b-a)(\ln b - \ln a)$ valid for an arbitrary pair of a and b , D_{KL} provides a lower bound on the entropy production $\langle \Sigma \rangle_0 = \int_0^{\tau_p} dt \sum_{i \neq j; \mu} p_j k_{ij}^\mu \ln[(p_j k_{ij}^\mu)/(p_i k_{ji}^\mu)]$, as given by Ref. [2],

$$D_{\text{KL}} \leq \frac{\theta^2}{4} \langle \Sigma \rangle_0. \quad (\text{S43})$$

Also, since $(b-a)^2/(a+b) \leq a+b$ for positive a and b , the KL divergence is also bounded by

$$D_{\text{KL}} \leq \frac{\theta^2}{2} \langle A \rangle_0, \quad (\text{S44})$$

with the average activity being $\langle A \rangle_0 = \int_0^{\tau_p} dt \sum_{i \neq j; \mu} (p_j k_{ij}^\mu + p_i k_{ji}^\mu)$.

Using the form of α_{ij}^μ , it is simple to show that [2], to the first order of θ ,

$$\begin{aligned} \hat{L}(\theta, t) |p(0, t)\rangle &= (1 + \theta) \hat{L}(0, t) |p(0, t)\rangle + \mathcal{O}(\theta^2) \\ &= (1 + \theta) \partial_t |p(0, t)\rangle + \mathcal{O}(\theta^2). \end{aligned} \quad (\text{S45})$$

By applying $\hat{L}^+(\theta, t)$ on both sides, we have

$$|p(0, t)\rangle = |\pi(\theta, t)\rangle + (1 + \theta) \hat{L}^+(\theta, t) |\partial_t p(0, t)\rangle. \quad (\text{S46})$$

By applying the adiabatic perturbation method, we derive $|p(0, t)\rangle = |\pi(\theta, t)\rangle + (1 + \theta) \hat{L}^+(\theta, t) |\pi(\theta, t)\rangle + (1 + \theta)^2 \hat{L}^+(\theta, t) \partial_t (\hat{L}^+(\theta, t) |\partial_t \pi(\theta, t)\rangle) + \mathcal{O}(\theta^2) = |p(\theta, t)\rangle + \theta |p_{\text{curv}}(\theta, t)\rangle + 2\theta |p_{\text{metr}}(\theta, t)\rangle + \mathcal{O}(\theta^2)$. Therefore, we have

$$\begin{aligned} \partial_\theta |p(\theta, t)\rangle|_{\theta \rightarrow 0} &= \lim_{\theta \rightarrow 0} \frac{|p(\theta, t)\rangle - |p(0, t)\rangle}{\theta} \\ &= -|p_{\text{curv}}(0, t)\rangle - 2|p_{\text{metr}}(0, t)\rangle. \end{aligned} \quad (\text{S47})$$

Also, we can obtain $\langle 1 | \partial_\theta \hat{J}(\theta) |_{\theta \rightarrow 0} |p(0, t)\rangle = \langle 1 | \hat{J}(0, t) |p(0, t)\rangle$ by using the form of the perturbed transition rates $k_{ij}^\mu(\theta, t)$.

In this way, we show that the linear response of $\langle Q \rangle$ due to the perturbation is given by

$$\begin{aligned} \lim_{\theta \rightarrow 0} \frac{\langle Q \rangle_\theta - \langle Q \rangle_0}{\theta} &= \int_0^{\tau_p} dt \partial_\theta \langle 1 | \hat{J}(\theta, t) |p(\theta, t)\rangle|_{\theta \rightarrow 0} \\ &= \langle Q_{\text{dyn}} \rangle_0 - \langle Q_{\text{metr}} \rangle_0. \end{aligned} \quad (\text{S48})$$

According to the linear fluctuation-response inequality $(\langle Q \rangle_\theta - \langle Q \rangle_0)^2 \leq 2D_{\text{KL}} \langle Q^2 \rangle_c$, first propose by Ref. [2], we reach the final result

$$\langle \Sigma \rangle \langle Q^2 \rangle_c \geq 2(\langle Q_{\text{dyn}} \rangle - \langle Q_{\text{metr}} \rangle)^2, \quad (\text{S49})$$

where we omit the subscript 0 since all averages are with regard to the unperturbed dynamics. The average entropy production is thus bounded by Σ_g

$$\langle \Sigma \rangle \geq \frac{2(\langle Q_{\text{dyn}} \rangle - \langle Q_{\text{metr}} \rangle)^2}{\langle Q^2 \rangle_c} := \Sigma_g. \quad (\text{S50})$$

This is the so called Geometric TURs, one of our main results.

Similarly, the average activity is bounded by

$$\langle A \rangle \geq \frac{(\langle Q_{\text{dyn}} \rangle - \langle Q_{\text{metr}} \rangle)^2}{\langle Q^2 \rangle_c} := A_g. \quad (\text{S51})$$

We further discuss some consequences of Eq. (S49). If the instantaneous steady state $|\pi(t)\rangle$ is actually the equilibrium state, the dynamic part $\langle \Sigma_{\text{dyn}} \rangle$ and $\langle Q_{\text{dyn}} \rangle$ and the adiabatic curvature part $\langle \Sigma_{\text{curv}} \rangle$ vanish. The TUR simplifies to

$$\langle \Sigma_{\text{metr}} \rangle \langle Q^2 \rangle_c \geq 2 \langle Q_{\text{metr}} \rangle^2. \quad (\text{S52})$$

If we consider the current Q to be Σ , this inequality further simplifies to

$$\langle \Sigma^2 \rangle_c \geq 2 \langle \Sigma_{\text{metr}} \rangle \geq \frac{2\mathcal{L}^2}{\tau_p}, \quad (\text{S53})$$

bounding the fluctuation of entropy production with the thermodynamic length given by the metric of $\langle \Sigma_{\text{metr}} \rangle$, i.e., for $\langle \Sigma_{\text{metr}} \rangle = \int_0^{\tau_p} dt g_{\mu\nu}^{\Sigma} \dot{\Lambda}_\mu \dot{\Lambda}_\nu$, $\mathcal{L} := \oint_{\partial\Omega} dt \sqrt{g_{\mu\nu}^{\Sigma} \dot{\Lambda}_\mu \dot{\Lambda}_\nu}$. Here, the second inequality can actually be saturated by optimizing the parametrization of protocol. We note \mathcal{L} is independent of the detailed protocol but only dependent on the path in the parameter space. According to this inequality, the underlying thermodynamic length is bounded from above by an arbitrary parametrization of the path in the parameter space

$$\mathcal{L} \leq \sqrt{\tau_p \langle \Sigma^2 \rangle_c} / 2. \quad (\text{S54})$$

This form a basis for future inference of the thermodynamic length.

VI. MODELS

We treat the theoretical details of our two models with continuous and discrete degrees of freedom in this section.

A. Chiral current in the nonequilibrium tricycle

We consider a system composed of three quantum dots with tunable energy levels. Electrons can tunnel between one of

the dots and an electron thermal reservoir. We also indirectly couple these dots with three photonic/phononic baths. The bosonic baths compensate the energy difference between dots and renders the system a nonequilibrium quantum tricycle. To be specific, the system Hamiltonian $\hat{H} = \hat{H}_S + \hat{H}_R + \hat{H}_{SR} + \hat{H}_B + \hat{H}_{SB}$ is composed of the three quantum dot levels $\hat{H}_S = \sum_{n=1}^3 \epsilon_n \hat{c}_n^\dagger \hat{c}_n$, the electron reservoirs $\hat{H}_R = \sum_k \epsilon_k \hat{d}_k^\dagger \hat{d}_k$, the tunneling term $\hat{H}_{SR} = \sum_k t_k (\hat{d}_k^\dagger \hat{c}_3 + \hat{c}_3^\dagger \hat{d}_k)$, the Bosonic thermal bath $\hat{H}_B = \sum_{\nu=1; k}^{\nu=3} \epsilon_{\nu, k} \hat{a}_{\nu, k}^\dagger \hat{a}_{\nu, k}$, and the system-bath coupling term $\hat{H}_{SB} = \sum_{\nu=1; k}^{\nu=3} r_{\nu, k} (\hat{a}_{\nu, k} + \hat{a}_{\nu, k}^\dagger) (\hat{c}_\nu^\dagger \hat{c}_{\nu+1} + \hat{c}_{\nu+1}^\dagger \hat{c}_\nu)$. Here, $\nu = 4$ denotes the same site as $\nu = 1$. We restrict ourselves to the weak coupling regime. Under the standard Born-Markov approximation, we obtain the transition rates between different states.

By concentrating on the strong Coulomb blockade regime, the master equation is $\partial_t |p_{\mathcal{X}}\rangle = \hat{L}_{\mathcal{X}} |p_{\mathcal{X}}\rangle$, with $|p\rangle = (p_0, p_1, p_2, p_3)^T$ and

$$\hat{L}_{\mathcal{X}} = \begin{pmatrix} -k_+ & 0 & 0 & k_- e^{\chi_2(\epsilon_3 - \mu)/T_R} \\ 0 & -(k_{21} + k_{31}) & k_{12} e^{\chi_2(\epsilon_2 - \epsilon_1)/T_1} & k_{13} e^{-\chi_1 + \chi_2(\epsilon_3 - \epsilon_1)/T_3} \\ 0 & k_{21} e^{-\chi_2(\epsilon_2 - \epsilon_1)/T_1} & -(k_{12} + k_{32}) & k_{23} e^{\chi_2(\epsilon_3 - \epsilon_2)/T_2} \\ k_+ e^{-\chi_2(\epsilon_3 - \mu)/T_R} & k_{31} e^{\chi_1 - \chi_2(\epsilon_3 - \epsilon_1)/T_3} & k_{32} e^{-\chi_2(\epsilon_3 - \epsilon_2)/T_2} & -(k_- + k_{13} + k_{23}) \end{pmatrix}, \quad (\text{S55})$$

where k_{ij} represents the transition from j to i . To be concrete, we suppose $\epsilon_3 > \epsilon_2 > \epsilon_1$. Here, the rates $\Gamma_R = 2\pi \sum_k t_k^2 \delta(\epsilon - \epsilon_k)$ and $\Gamma_\nu = 2\pi \sum_k r_{\nu, k}^2 \delta(\epsilon - \epsilon_{\nu, k})$ are taken as constant under the flat-band limit. $f(\epsilon) = 1/[e^{(\epsilon - \mu)/T_R} + 1]$ and $n_\nu(\epsilon) = 1/(e^{\epsilon/T_\nu} - 1)$ are respectively the Fermi and Bose distribution.

$$\begin{aligned} k_+ &= \Gamma_R f(\epsilon_3), \\ k_- &= \Gamma_R [1 - f(\epsilon_3)], \end{aligned} \quad (\text{S56})$$

$$\begin{aligned} k_{21} &= \Gamma_1 n_1(\epsilon_2 - \epsilon_1), \\ k_{12} &= \Gamma_1 [1 + n_1(\epsilon_2 - \epsilon_1)], \end{aligned} \quad (\text{S57})$$

$$\begin{aligned} k_{32} &= \Gamma_2 n_2(\epsilon_3 - \epsilon_2), \\ k_{23} &= \Gamma_2 [1 + n_2(\epsilon_3 - \epsilon_2)], \end{aligned} \quad (\text{S58})$$

$$\begin{aligned} k_{31} &= \Gamma_3 n_3(\epsilon_3 - \epsilon_1), \\ k_{13} &= \Gamma_3 [1 + n_3(\epsilon_3 - \epsilon_1)]. \end{aligned} \quad (\text{S59})$$

We use χ_1 to count the chiral current and χ_2 to count the entropy production.

Similarly, with regard to the dynamic activity of the whole system, which is the total number of bidirectional transitions between each pair of states, we can also count it with χ_3 , with the corresponding

$$\hat{L}_{\mathcal{X}} = \begin{pmatrix} -k_+ & 0 & 0 & k_- e^{\chi_3} \\ 0 & -(k_{21} + k_{31}) & k_{12} e^{\chi_3} & k_{13} e^{\chi_3} \\ 0 & k_{21} e^{\chi_3} & -(k_{12} + k_{32}) & k_{23} e^{\chi_3} \\ k_+ e^{\chi_3} & k_{31} e^{\chi_3} & k_{32} e^{\chi_3} & -(k_- + k_{13} + k_{23}) \end{pmatrix}, \quad (\text{S60})$$

We drive the system according to the protocol $\epsilon_3(t) = 1 + \delta \sin(2\pi t/\tau_p)$, $\epsilon_2(t) = 0.5 + \delta \sin(2\pi t/\tau_p + \phi)$, $\epsilon_1(t) = \delta \sin(2\pi t/\tau_p + 2\phi)$ ($0 \leq \delta < 0.25$), and $\Gamma_\nu = \Gamma_R = \Gamma$. The parameters δ , ϕ , τ_p , Γ_B , T_ν ($\nu = 1, 2, 3$), T_R and μ determine our model. The characteristic time scale of this system is $\tau_c \approx 1/\Gamma$. The pumped chiral current is shown in Fig. S2. $T_3 = 1.00$ corresponds to the case with no dynamic components.

In the Fig. 2(c) of the main text, we select $T_1 = T_2 = T_R = 1$, $\mu = 5$, the period $10^{1/2} \leq \tau_p \leq 100$, the driving amplitude $\delta = 0.2$, the temperature $0.97 \leq T_3 \leq 1.03$ and the phase difference $0 \leq \phi \leq 2\pi$.

In the Fig. 2(d) of the main text, we select the temperatures all being $T_1 = T_2 = T_3 = T_R = 1$, $\mu = 5$, the driving amplitude $\delta \in \{0.05, 0.10, 0.15, 0.20\}$ and the phase difference $0 \leq \phi \leq 2\pi$.

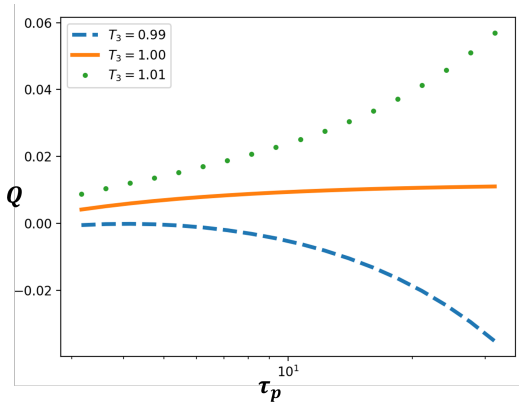


FIG. S2. **The nonequilibrium chiral current versus the driving period.** $T_3 = 1.00$ has no dynamic component and other two systems have nonzero dynamic chiral current. Here, the parameters are given by $\phi = 2\pi/3$, $\delta = 0.2$, $T_1 = T_2 = T_R = 1.00$, and $\mu = 5.0$.

B. Brownian heat pump

Consider a harmonic oscillator composed of two particles coupling two reservoirs, which is illustrated in Fig. S3(a). The Langevin equation of motion is given by

$$\begin{aligned} \gamma_1 \dot{x}_1 &= k(x_2 - x_1) + \xi_1, \\ \gamma_2 \dot{x}_2 &= k(x_1 - x_2) + \xi_2, \end{aligned} \quad (\text{S61})$$

where k is the stiffness of the oscillator and ξ_i is the Gaussian white noise satisfying $\langle \xi_i(t_1)\xi_j(t_2) \rangle = 2\gamma_i T_i \delta_{ij} \delta(t_1 - t_2)$. Due to the translational invariance of the above equations, it is equivalent to the dynamics of a single overdamped oscillator $\gamma \dot{y} = -ky + \xi(t)$, with $y = x_1 - x_2$ being the effective degree of freedom, $\gamma = \gamma_1 \gamma_2 / (\gamma_1 + \gamma_2)$, and $\xi = (\gamma_2 \xi_1 - \gamma_1 \xi_2) / (\gamma_1 + \gamma_2)$. We note the effective noise ξ has zero mean and the variance $\langle \xi(t_1)\xi(t_2) \rangle = 2\gamma T_e \delta(t_1 - t_2)$, with the effective temperature given by $T_e = (\gamma_2 T_1 + \gamma_1 T_2) / (\gamma_1 + \gamma_2)$.

Here, the stochastic heat flowing into the system from the first reservoir is $\dot{Q}_1 = (-\gamma_1 \dot{x}_1 + \xi_1) \dot{x}_1 = -\frac{k^2}{\gamma_1} y^2 + \frac{k}{\gamma_1} \xi_1 y$, and

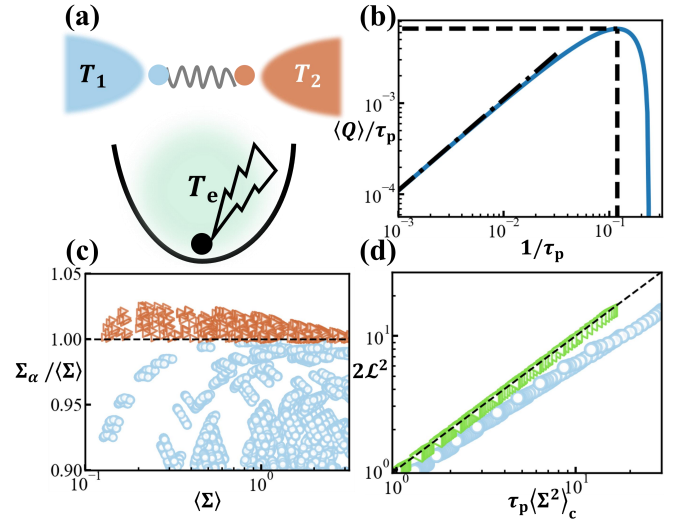


FIG. S3. **The Brownian heat pump model by cyclically driving the stiffness of the oscillator k and the coupling to the left reservoir γ_1 .** (a) The Brownian model and its effective system. (b) The geometrically pumped heat density Q/τ versus the inverse period $1/\tau_p$ (the solid line). Here, we choose the protocol $k(t)/k_0 = 1 + \sin(2\pi t/\tau_p)/2$, $\gamma_1(t)/\gamma_2 = 1 + \sin(2\pi t/\tau_p + \pi/2)/2$ and $T_1 = T_2$, with k_0 being a stiffness constant. The dot-dash line is for the adiabatic component $\langle Q_{\text{curv}} \rangle / \tau_p$ and the dash line denotes the optimal driving period. (c) The thermodynamic uncertainty relations ($\Sigma_\alpha = \Sigma_b$ or Σ_g). Our geometric bound $\langle \Sigma \rangle \geq \Sigma_g$ is satisfied (blue circles), while the steady state bound $\langle \Sigma \rangle \geq \Sigma_b$ can be broken (orange triangles); we only show the breaking situations of the latter bound for clarity. (d) The geometric bound of the fluctuation of the entropy production (Eq. (S53)). Blue circles are for constant speed driving protocols and green triangles (on the dashed line) are for the optimal protocols parametrized in terms of the length \mathcal{L} .

the stochastic entropy production rate $\dot{\Sigma} = -\dot{Q}_1/T_1 - \dot{Q}_2/T_2$ is given by

$$\dot{\Sigma} = \left(\frac{1}{\gamma_1 T_1} + \frac{1}{\gamma_2 T_2} \right) k^2 y^2 - \left(\frac{\xi_1}{\gamma_1 T_1} - \frac{\xi_2}{\gamma_2 T_2} \right) k y. \quad (\text{S62})$$

Defining the joint distribution function $|p(y, Q, \Sigma, t)\rangle$, its dynamics is governed by the stochastic Liouville equation $\partial_t |p(y, Q, \Sigma, t)\rangle = \hat{\Omega} |p(y, Q, \Sigma, t)\rangle$ following the continuity relation $\hat{\Omega} = -\partial_y \dot{y} - \partial_{Q_1} \dot{Q}_1 - \partial_\Sigma \dot{\Sigma}$. By taking an ensemble average over the reservoir noise, we derive the generalized Fokker-Planck operator as $\hat{L} = \lim_{\Delta t \rightarrow 0} \frac{1}{\Delta t} [\int_t^{t+\Delta t} dt_1 \langle \hat{\Omega}(t_1) \rangle + \int_t^{t+\Delta t} dt_1 \int_t^{t_1} dt_2 \langle \hat{\Omega}(t_1) \hat{\Omega}(t_2) \rangle]$. The first term is the ballistic term $\hat{L}_1 = \frac{k}{\gamma} \partial_y y + \frac{k^2}{\gamma_1} y^2 \partial_{Q_1} - \left(\frac{1}{\gamma_1 T_1} + \frac{1}{\gamma_2 T_2} \right) k^2 y^2 \partial_\Sigma$, while the second term is the diffusion term $\hat{L}_2 = \frac{T_e}{\gamma} \partial_y^2 + \frac{k T_1}{\gamma_1} (\partial_y y + y \partial_y) \partial_{Q_1} - \frac{k}{\gamma} (\partial_y y + y \partial_y) \partial_\Sigma - \frac{2k^2}{\gamma_1} y^2 \partial_{Q_1} \partial_\Sigma + \frac{k^2 T_1}{\gamma_1} y^2 \partial_{Q_1}^2 + \left(\frac{1}{\gamma_1 T_1} + \frac{1}{\gamma_2 T_2} \right) k^2 y^2 \partial_\Sigma^2$.

We use the counting field $\chi = (\chi_1, \chi_2)^T$ with two components generating the statistics of Q_1 and Σ respectively. By making a Fourier-Laplace transformation $|p(y, \chi, t)\rangle = \int dQ d\Sigma |p(y, Q, \Sigma, t)\rangle e^{i\chi_1 Q + \chi_2 \Sigma}$, we derive

the twisted Fokker-Planck operator as a generator for the dynamics of $|p(y, \chi, t)\rangle$

$$\hat{L}_\chi = \frac{T_e}{\gamma} \partial_y^2 + a_1 y \partial_y + a_2 y^2 + a_3, \quad (\text{S63})$$

with the coefficients $a_1 = \frac{k}{\gamma}[1 + 2(\chi_2 - \frac{\gamma}{\gamma_1} T_1 \chi_1)]$, $a_2 = k^2[\frac{\chi_1}{\gamma_1}(T_1 \chi_1 - 1) + (\frac{1}{\gamma_1 T_1} + \frac{1}{\gamma_2 T_2})\chi_2(\chi_2 + 1) - \frac{2}{\gamma_1} \chi_1 \chi_2]$ and $a_3 = \frac{k}{\gamma}(1 + \chi_2 - \frac{\gamma}{\gamma_1} T_1 \chi_1)$. A similarity transformation $\hat{U} = e^{\beta k y^2/2}$ would bring \hat{L}_χ into a Hermitian operator $\tilde{L}_\chi = \tilde{L}_\chi^\dagger = \hat{U} \hat{L}_\chi \hat{U}^{-1} = \frac{T_e}{\gamma} \partial_y^2 + (a_2 - \frac{a_1^2 \gamma}{4 T_e}) y^2 + (a_3 - \frac{a_1}{2})$, where $\beta = \frac{a_1 \gamma}{2 T_e k}$.

Analogous to the solution of quantum oscillators, in terms of the lowering $\hat{b} = \sqrt{\epsilon} \partial_y + \frac{1}{2\sqrt{\epsilon}} y$ and raising operator $\hat{b}^\dagger = -\sqrt{\epsilon} \partial_y + \frac{1}{2\sqrt{\epsilon}} y$ ($[\hat{b}, \hat{b}^\dagger] = 1$), where the factor $\epsilon = \frac{T_e}{\sqrt{a_1^2 \gamma^2 - 4 a_2 T_e \gamma}}$, we can write $\tilde{L}_\chi = -\frac{T_e}{\gamma \epsilon} \hat{b}^\dagger \hat{b} + (a_3 - \frac{a_1}{2} - \frac{T_e}{2 \gamma \epsilon})$. Therefore, we derive the eigenvalues of \hat{L}_χ to be $E_n = -n \frac{T_e}{\gamma \epsilon} + (a_3 - \frac{a_1}{2} - \frac{T_e}{2 \gamma \epsilon})$ (E_0 corresponding to the steady state) and the eigenvectors to be

$$|r_n\rangle = \hat{U}^{-1} |\psi_n\rangle = \frac{1}{\sqrt{n!}} \hat{U}^{-1} (\hat{b}^\dagger)^n |\psi_0\rangle, \quad (\text{S64})$$

$$\langle l_n | = \langle \psi_n | \hat{U} = \frac{1}{\sqrt{n!}} \langle \psi_0 | \hat{b}^n \hat{U},$$

where $|\psi_0\rangle = (|\langle \psi_0 | \rangle)^\dagger$ is the ground eigenstate of \tilde{L}_χ satisfying $\hat{b} |\psi_0\rangle = 0$. Here, $\{|\psi_n\rangle\}$ forms an orthonormal basis $\langle \psi_m | \psi_n \rangle = \delta_{mn}$.

The ground state satisfies $\hat{b} |\psi_0\rangle = 0$ ($(\sqrt{\epsilon} \partial_y + \frac{1}{2\sqrt{\epsilon}} y) |\psi_0\rangle = 0$) and is thus given by a Gaussian distribution [5]

$$|\psi_0\rangle = \left(\frac{1}{2\pi\epsilon}\right)^{1/4} e^{-\frac{y^2}{4\epsilon}}, \quad (\text{S65})$$

with an expression similar to the ground state wavefunction of the quantum harmonic oscillator. To calculate the geometric CGF, we note the relations $y = \sqrt{\epsilon}(\hat{b} + \hat{b}^\dagger)$, $|\partial_\mu \psi_0\rangle = \frac{(y^2 - \epsilon) \partial_\mu \epsilon}{4\epsilon^2} |\psi_0\rangle$, $\partial_\mu \hat{U} = (\partial_\mu \beta k) \frac{y^2}{2} \hat{U}$ and $\partial_\mu \hat{U}^{-1} = -(\partial_\mu \beta k) \frac{y^2}{2} \hat{U}^{-1}$. We show

$$\begin{aligned} |\partial_\mu r_0\rangle &= -\frac{\epsilon \partial_\mu (\beta k)}{2} |r_0\rangle + \sqrt{2} \left[\frac{\partial_\mu \epsilon}{4\epsilon} - \frac{\epsilon \partial_\mu (\beta k)}{2} \right] |r_2\rangle, \\ \langle \partial_\mu l_0 | &= \frac{\epsilon \partial_\mu (\beta k)}{2} \langle l_0 | + \sqrt{2} \left[\frac{\partial_\mu \epsilon}{4\epsilon} + \frac{\epsilon \partial_\mu (\beta k)}{2} \right] \langle l_2 |. \end{aligned} \quad (\text{S66})$$

The relation $\langle l_0 | \partial_\mu r_0 \rangle + \langle \partial_\mu l_0 | r_0 \rangle = 0$ is satisfied due to the normalization condition $\langle l_0 | r_0 \rangle = 1$. For arbitrary driven parameters, the geometric connection is $A_\mu = -\langle l_0 | \partial_\mu r_0 \rangle = \epsilon \partial_\mu (\beta k) / 2$. The corresponding geometric curvature is $F_{\mu\nu} = \partial_\mu A_\nu - \partial_\nu A_\mu = [(\partial_\mu \epsilon)(\partial_\nu \beta k) - (\partial_\nu \epsilon)(\partial_\mu \beta k)] / 2$. The metric tensor is given by

$$g_{\mu\nu} = \frac{\gamma}{16 T_e \epsilon} [4\epsilon^4 (\partial_\mu \beta k)(\partial_\nu \beta k) - (\partial_\mu \epsilon)(\partial_\nu \epsilon)]. \quad (\text{S67})$$

To illustrate our theory, we consider a heat engine powered by driving k and γ_1 , i.e. $\Lambda = (k, \gamma_1)^T$. We first consider

the driving protocol $k = k_0[1 + a \sin(2\pi t/\tau_p)]$, $\gamma_1 = \gamma_0[1 + a \sin(2\pi t/\tau_p + \phi)]$, and $\gamma_2 = \gamma_0$. The parameters τ_p , T_1 , T_2 and ϕ can be taken as configurations of the driving protocol. We further define a time scale of this system as $\tau_c = \gamma_0/k_0$, which is of the same order of the characteristic time scale γ/k .

The instantaneous dynamic components for $\langle Q \rangle$, $\langle Q^2 \rangle_c$, $\langle \Sigma \rangle$ and $\langle \Sigma^2 \rangle_c$ are given by

$$E^Q := \partial_{\chi_1} E_0|_{\chi=0} = \frac{1}{\tau_c} \frac{\tilde{k}(T_1 - T_2)}{\tilde{\gamma}_1 + 1}, \quad (\text{S68})$$

$$E^{Q^2} := \partial_{\chi_1}^2 E_0|_{\chi=0} = \frac{1}{\tau_c} \frac{2\tilde{k}(T_2 \tilde{\gamma}_1 + T_1)(T_1 \tilde{\gamma}_1 + T_2)}{(\tilde{\gamma}_1 + 1)^3}, \quad (\text{S69})$$

$$E^\Sigma := \partial_{\chi_2} E_0|_{\chi=0} = \frac{1}{\tau_c} \frac{\tilde{k}(T_1 - T_2)^2}{T_1 T_2 (\tilde{\gamma}_1 + 1)}, \quad (\text{S70})$$

$$\begin{aligned} E^{\Sigma^2} &:= \partial_{\chi_2}^2 E_0|_{\chi=0} \\ &= \frac{1}{\tau_c} \frac{2\tilde{k}(T_1 - T_2)^2 [T_1^2 \tilde{\gamma}_1 + T_2^2 \tilde{\gamma}_1 + T_1 T_2 (\tilde{\gamma}_1^2 + 1)]}{T_1^2 T_2^2 (\tilde{\gamma}_1 + 1)^3}, \end{aligned} \quad (\text{S71})$$

where we define the dimensionless factors $\tilde{k} := k/k_0$ and $\tilde{\gamma}_1 := \gamma_1/\gamma_0$.

The geometric connection vectors for $\langle Q_{\text{curv}} \rangle$, $\langle Q_{\text{curv}}^2 \rangle_c$ and $\langle \Sigma_{\text{curv}} \rangle$ are given by

$$A_\mu^Q d\Lambda_\mu = -\frac{(T_2 \tilde{\gamma}_1 + T_1)}{2\tilde{k}(\tilde{\gamma}_1 + 1)^2} d\tilde{k} + \frac{T_1 \tilde{\gamma}_1 + T_2}{2(\tilde{\gamma}_1 + 1)^3} d\tilde{\gamma}_1, \quad (\text{S72})$$

$$\begin{aligned} A_\mu^{Q^2} d\Lambda_\mu &= \frac{\tilde{\gamma}_1 (T_2 \tilde{\gamma}_1 + T_1) [T_1 (\tilde{\gamma}_1 - 2) + 3T_2]}{\tilde{k}(\tilde{\gamma}_1 + 1)^4} d\tilde{k} \\ &+ \frac{3\tilde{\gamma}_1 (T_1 - T_2) (T_1 \tilde{\gamma}_1 + T_2)}{(\tilde{\gamma}_1 + 1)^5} d\tilde{\gamma}_1, \end{aligned} \quad (\text{S73})$$

$$\begin{aligned} A_\mu^\Sigma d\Lambda_\mu &= \frac{(T_2 \tilde{\gamma}_1 + T_1) (T_1 \tilde{\gamma}_1 + T_2)}{2\tilde{k} T_1 T_2 (\tilde{\gamma}_1 + 1)^2} d\tilde{k} \\ &+ \frac{(T_1 - T_2) (T_1 \tilde{\gamma}_1 + T_2)}{2T_1 T_2 (\tilde{\gamma}_1 + 1)^3} d\tilde{\gamma}_1, \end{aligned} \quad (\text{S74})$$

$$\begin{aligned} A_\mu^{\Sigma^2} d\Lambda_\mu &= \frac{3(T_1 - T_2)^2 (T_1 \tilde{\gamma}_1 + T_2)}{T_1^2 T_2^2 (\tilde{\gamma}_1 + 1)^4} \left[\frac{\tilde{\gamma}_1 (T_2 \tilde{\gamma}_1 + T_1)}{\tilde{k}} d\tilde{k} \right. \\ &+ \left. \frac{(T_1 - T_2) \tilde{\gamma}_1}{\tilde{\gamma}_1 + 1} d\tilde{\gamma}_1 \right]. \end{aligned} \quad (\text{S75})$$

Obviously, from Eq. (S70), Eq. (S71), Eq. (S74) and Eq. (S75), we can easily show that both the dynamic and adiabatic geometric components of the entropy production (and its variance) vanish in the isothermal case where $T_1(t) = T_2(t)$. Particularly, although $A_{\mu\nu}^\Sigma d\Lambda_\mu \neq 0$ in this situation, it simplifies to $\frac{1}{2} d \ln \tilde{k}$ as a total derivative of \tilde{k} and therefore the accumulation during one cycle $\int_{\partial\Omega} A_{\mu\nu}^\Sigma d\Lambda_\mu$ is zero.

The geometric metrics are given by

$$\mathfrak{g}_{\mu\nu}^Q d\Lambda_\mu d\Lambda_\nu = \frac{\tau_c \tilde{\gamma}_1}{4\tilde{k}^3(\tilde{\gamma}_1 + 1)^3} [-(T_2 \tilde{\gamma}_1 + T_1)(d\tilde{k})^2 + \tilde{k} T_2 d\tilde{k} d\tilde{\gamma}_1 + \frac{\tilde{k}^2 (T_1 - T_2)}{(\tilde{\gamma}_1 + 1)^2} (d\tilde{\gamma}_1)^2], \quad (\text{S76})$$

$$\begin{aligned} \mathfrak{g}_{\mu\nu}^{Q^2} d\Lambda_\mu d\Lambda_\nu = & \tau_c \left[\frac{\tilde{\gamma}_1 (T_2 \tilde{\gamma}_1 + T_1) [6T_2 \tilde{\gamma}_1 + T_1 (\tilde{\gamma}_1^2 - 4\tilde{\gamma}_1 + 1)]}{2\tilde{k}^3 (\tilde{\gamma}_1 + 1)^5} (d\tilde{k})^2 - \frac{T_2 \tilde{\gamma}_1 [6T_2 \tilde{\gamma}_1 + T_1 (\tilde{\gamma}_1^2 - 4\tilde{\gamma}_1 + 1)]}{2\tilde{k}^2 (\tilde{\gamma}_1 + 1)^5} d\tilde{k} d\tilde{\gamma}_1 \right. \\ & \left. - \frac{\tilde{\gamma}_1 [T_1 T_2 (-3\tilde{\gamma}_1^2 + 14\tilde{\gamma}_1 - 3) + T_1^2 (\tilde{\gamma}_1^2 - 8\tilde{\gamma}_1 + 1) + T_2^2 (\tilde{\gamma}_1^2 - 8\tilde{\gamma}_1 + 1)]}{2\tilde{k} (\tilde{\gamma}_1 + 1)^7} (d\tilde{\gamma}_1)^2 \right], \end{aligned} \quad (\text{S77})$$

$$\mathfrak{g}_{\mu\nu}^\Sigma d\Lambda_\mu d\Lambda_\nu = \tau_c \left[\frac{\tilde{\gamma}_1 (T_2 \tilde{\gamma}_1 + T_1) (T_1 \tilde{\gamma}_1 + T_2)}{4\tilde{k}^3 T_1 T_2 (\tilde{\gamma}_1 + 1)^3} (d\tilde{k})^2 + \frac{(T_1^2 - T_2^2) \tilde{\gamma}_1}{4\tilde{k}^2 T_1 T_2 (\tilde{\gamma}_1 + 1)^3} d\tilde{k} d\tilde{\gamma}_1 + \frac{(T_1 - T_2)^2 \tilde{\gamma}_1}{4\tilde{k} T_1 T_2 (\tilde{\gamma}_1 + 1)^5} (d\tilde{\gamma}_1)^2 \right], \quad (\text{S78})$$

$$\begin{aligned} \mathfrak{g}_{\mu\nu}^{\Sigma^2} d\Lambda_\mu d\Lambda_\nu = & \tau_c \left[\frac{\tilde{\gamma}_1 (T_2 \tilde{\gamma}_1 + T_1) [6T_1^3 \tilde{\gamma}_1^2 + 6T_2^3 \tilde{\gamma}_1 + T_1 T_2^2 (7\tilde{\gamma}_1^2 - 10\tilde{\gamma}_1 + 1) + T_1^2 T_2 \tilde{\gamma}_1 (\tilde{\gamma}_1^2 - 10\tilde{\gamma}_1 + 7)]}{2\tilde{k}^3 T_1^2 T_2^2 (\tilde{\gamma}_1 + 1)^5} (d\tilde{k})^2 \right. \\ & + \frac{\tilde{\gamma}_1 (T_1^2 - T_2^2) [6T_1^2 \tilde{\gamma}_1 + 6T_2^2 \tilde{\gamma}_1 + T_1 T_2 (\tilde{\gamma}_1^2 - 10\tilde{\gamma}_1 + 1)]}{2\tilde{k}^2 T_1^2 T_2^2 (\tilde{\gamma}_1 + 1)^5} d\tilde{k} d\tilde{\gamma}_1 \\ & \left. + \frac{\tilde{\gamma}_1 (T_1 - T_2)^2 [T_1 T_2 (3\tilde{\gamma}_1^2 - 14\tilde{\gamma}_1 + 3) - T_1^2 (\tilde{\gamma}_1^2 - 8\tilde{\gamma}_1 + 1) - T_2^2 (\tilde{\gamma}_1^2 - 8\tilde{\gamma}_1 + 1)]}{2\tilde{k} T_1^2 T_2^2 (\tilde{\gamma}_1 + 1)^7} (d\tilde{\gamma}_1)^2 \right]. \end{aligned} \quad (\text{S79})$$

In the non-biased situation, $T_1 = T_2$ and the metric structure for $\langle \Sigma \rangle$ and $\langle \Sigma^2 \rangle_c$ simplifies to be

$$\begin{aligned} \mathfrak{g}_{\mu\nu}^\Sigma d\Lambda_\mu d\Lambda_\nu &= \tau_c \frac{\tilde{\gamma}_1}{4\tilde{k}^3 (\tilde{\gamma}_1 + 1)} (d\tilde{k})^2, \\ \mathfrak{g}_{\mu\nu}^{\Sigma^2} d\Lambda_\mu d\Lambda_\nu &= 2(\mathfrak{g}_\Sigma)_{\mu\nu} d\Lambda_\mu d\Lambda_\nu. \end{aligned} \quad (\text{S80})$$

In this Brownian model, as an illustration, the metric structure of the average and variance of entropy production is of the form that our bound Eq. (S53) can actually be saturated. In numerical simulation, we randomly choose $10^{1/2} \leq \tau_p \leq 100$, $T_1 = 1$, $0.1 \leq T_2 \leq 1.9$, the driving amplitude $a = 0.5$ and the phase difference $0 \leq \phi \leq 2\pi$. The results validate the Geometric TURs in Fig S3(c).

To consider the geometric bound on the variance of entropy production in Fig. S3(d), we fix $T_1 = T_2 = 1$ and select the driving amplitude $a \in [0.4, 0.9]$ and the phase difference $0 \leq \phi \leq 2\pi$.

As shown in Fig. S3(b), the nonadiabatic heat pump effect is bounded from above by $\langle Q \rangle_{\text{curv}} / \tau_p$. We can eas-

ily show that the average heat flux $\langle Q \rangle / \tau_p$ reaches its maximum $-\langle Q_{\text{curv}} \rangle^2 / (4\tau_p \langle Q_{\text{metr}} \rangle)$ at the optimal period $-2\tau_p \langle Q_{\text{metr}} \rangle / \langle Q_{\text{curv}} \rangle$. In Fig. S3(c), independent of the driving protocols, the entropy production $\langle \Sigma \rangle$ is bounded from below by Σ_g (blue circles) as derived in Eq. (S50), but breaks the corresponding steady state bound $\langle \Sigma \rangle \geq \Sigma_b := 2 \langle Q \rangle^2 / \langle Q^2 \rangle_c$ (orange triangles). Furthermore, in this system, the metric expression for the average of entropy production $\mathfrak{g}_{\mu\nu}^\Sigma$ and entropy variance $\mathfrak{g}_{\mu\nu}^{\Sigma^2}$ for $T_1 = T_2$, i.e. Eq. (S79), satisfies

$$\mathfrak{g}_{\mu\nu}^{\Sigma^2} = 2\mathfrak{g}_{\mu\nu}^\Sigma = \frac{\gamma_1 \gamma_2}{2\tilde{k}^3 (\gamma_1 + \gamma_2)} \begin{pmatrix} 1 & 0 \\ 0 & 0 \end{pmatrix}, \quad (\text{S81})$$

implying that our geometric bound Eq. (S53) is actually saturable by reparametrizing the protocol in terms of the thermodynamic length, i.e. the time spend around a parameter point $dt = (\tau_p / \mathcal{L}) \sqrt{\mathfrak{g}_{\mu\nu}^\Sigma d\Lambda_\mu d\Lambda_\nu}$ [6, 7], as shown by the green triangles in Fig. S3(d). Here, $\mathfrak{g}_{\mu\nu}^\Sigma := \partial_{\chi_2} \mathfrak{g}_{\mu\nu} |_{\chi=0}$ and $\mathfrak{g}_{\mu\nu}^{\Sigma^2} := \partial_{\chi_2}^2 \mathfrak{g}_{\mu\nu} |_{\chi=0}$. The blue circles in Fig. S3(d) shows the validity of Eq. (S53) in the constant speed protocols.

-
- [1] T. R. Gingrich, G. M. Rotskoff, and J. M. Horowitz, Inferring dissipation from current fluctuations, *J. Phys. A* **50**, 184004 (2017).
 [2] A. Dechant and S.-i. Sasa, Fluctuation–response inequality out of equilibrium, *Proc. Natl. Acad. Sci. U.S.A.* **117**, 6430 (2020).
 [3] K. Liu, Z. Gong, and M. Ueda, Thermodynamic uncertainty relation for arbitrary initial states, *Phys. Rev. Lett.* **125**, 140602

- (2020).
 [4] T. Koyuk and U. Seifert, Thermodynamic uncertainty relation for time-dependent driving, *Phys. Rev. Lett.* **125**, 260604 (2020).
 [5] J. Ren, S. Liu, and B. Li, Geometric heat flux for classical thermal transport in interacting open systems, *Phys. Rev. Lett.* **108**, 210603 (2012).

- [6] G. E. Crooks, Measuring thermodynamic length, *Phys. Rev. Lett.* **99**, 100602 (2007).
- [7] K. Brandner and K. Saito, Thermodynamic geometry of microscopic heat engines, *Phys. Rev. Lett.* **124**, 040602 (2020).